The United Nations University
FISHERIES TRAINING PROGRAMME
P.O. Box 1390, Skulagata 4
120 Reykjavik, Iceland

Final Project 2003

REMOTE SENSING AND GEOGRAPHIC INFORMATION SYSTEM FOR PELAGIC FISHING GROUND FORECASTING IN NORTH ICELANDIC WATERS

Edgar Edmundo Lanz Sánchez
Instituto Tecnológico del Mar 03
Km. 4.5 Carretera al Varadero Nacional, Sector Playitas
Guaymas, Sonora, México
edgarlanz@yahoo.com

Supervisors
Geir Oddsson and Héðinn Valdimarsson
geiro@hi.is and hv@hafro.is

ABSTRACT

Fishing ground forecasting is gaining popularity in the fishing industries of many countries around the world. The managers of these fisheries want to know the status of the exploited fish stock and fishing grounds in order to optimise efforts and maintain sustainable commercial fisheries. Among the commercial marine species, small pelagic fish like sardine, jack mackerel and anchovy, are limited in their distribution by their temperature tolerance and by food availability, and they are in many ways, the most predictable fish species because of their behaviour. At the present time, modern technologies such as remotely sensed images obtained from aircraft and satellites, enable the gathering of information about the climatic characteristics and productivity of large areas of the oceans in a short time and at relatively low cost. The present project involves several objectives and phases to meet the goal of developing a Geographic Information System (GIS) and Remote Sensing (RS) -based fishing ground forecasting in north Icelandic waters, with the intention of providing the basis for a sustainable fisheries in the area.

Key words: *phytoplankton pigment concentration; sea surface temperature; remote sensing, AVHRR; SeaWIFS; CPUE; Geographic Information Systems, Bayesian theory; Multi Criteria Evaluation; Fuzzy logic theory; Fishing ground forecasting.*

TABLE OF CONTENTS

LIST OF FIGURES

LIST OF TABLES

1 INTRODUCTION

1.1 Environmental variables and capelin behaviour

Variations in ocean conditions play a key role in natural fluctuations of fish stocks and in their vulnerability to harvesting (Anon 1993).Evidence to date suggests that environmental factors, such as sea surface temperature (SST) have the greatest impact on larval fish stages and fish distribution (COMS 1978). Nowadays, SST is a good indicator for fishing areas and has been used for decades by fishermen and researchers (Barbieri *et al*. 1990, González 1993, Yáñez *et al*. 1996, Yáñez *et al*. 1997).

In addition, thermal gradient (GRT) has been included in some studies as an indicator of thermal fronts and up welling areas, which are highly productive areas that sustain fish populations (Fernández and Pingree 1996, Olson *et al*. 1994, Podesta *et al*. 1993, Polovina 1997, Yáñez *et al*. 1996, Nieto 1999). Studies on tuna, and related scombroid fishes, indicate the existence of distinct physical and biological boundaries that promote or inhibit major abundances or aggregations of schools, individuals or some size groups, which depend on ocean processes such as fronts, thermoclynes and productive regions of the oceans (Glantz and Feingold 1990, Kanthi 2000). Generally, both fishermen and sea birds have learned to operate in the vicinity of fronts, since they indicate fish abundance.

Capelin is a pelagic, migratory, planktivorous fish, and is therefore particularly sensitive to the ever-changing hydro-biological conditions of the seas where they feed. In addition, changes of their physical and biological environment may have profound effects on their abundance, migration patterns, distribution, and growth. The migration and distribution of capelin is closely linked to the system of ocean currents, and consequently to the distribution of water masses of the Icelandic shelf and in the Iceland Sea. Vilhjálmsson (1994) concluded that the feeding migration of adult capelin to higher latitudes (72°N) during spring and early summer is linked to an east-west temperature gradient. Also, water temperature has been cited as a determinant of spawning location (Carscadden *et al* 1989). This can occur when water temperature is suitable (Nakashima and Wheeler 2002). Vilhjálmsson (1994) recorded the lowest and highest temperatures of spawning as 1.5 and 14.0° C and spawning appears to be more common at lower temperatures.

Regarding the abundance of capelin and hydrological conditions, Malmberg and Blindheim (1994) noted certain general similarities between variations in oceanographic conditions north of Iceland in spring on the one hand, and the biomass of adult capelin in the period 1978 to 1992 on the other. The low sea temperatures and zooplankton production from 1979 to 1981 and again in the early 1990s seemed to be associated with reduced capelin growth and recruitment (Vilhjálmsson 1994). Astthorsson and Gislason (1998) classified hydrographical conditions north of Iceland during the years 1970-1998 into two categories, cold and warm. They found that there is a significant, but somewhat weak, correlation between capelin weight-at-age in winter and the sea temperature north of Iceland in spring of the year before. Great environmental variability in the sea around Iceland is further manifested in catch data variability in the summer fishing season, showing variations, both of geographic position and catch rates (Vilhjálmsson, 1994).

1.2 The use of GIS and remote sensing in fisheries

It is widely accepted in marine biology that temperature is the primary limiting factor in the occurrence of marine fish species(Taylor *et al*. 1953) and that it has local short-term effects on patterns of fish distribution. In addition, phenomena such as up welling areas, ocean colour and the presence of large amounts of chlorophyll in the water have been found as indicators of areas of fish stock congregations and fish stocks migration (Mansor *et al*. 2001).

Oceanography based on remote sensing provides a method to collect global data on a regular basis; it supplies the possibility to monitor ocean surface or sub-surface dynamic variability and climate at the necessary spatial extension with multiple spectral data at relatively low-cost. Several sensors are now available for the monitoring of the marine environment and resources (Table 1). The SeaWiFS (Sea-viewing Wide-Field-of view Sensor) on board the SeaStar spacecraft is an advanced sensor designed for ocean monitoring. The SeaWIFS satellite, launched in September 1997, is capable of detecting sea-surface phytoplankton chlorophyll with ocean colour measurements for estimating total phytoplankton primary production in an effort to determine the role of the oceans in global climate change. In addition, the satellite sensor which measures SST best, the NOAA AVHRR, has a spatial resolution of 1.1 km and 4 km (LAC and GAC resolution, respectively),and is suitable for mesoscale and global scale thermal monitoring in the ocean.

Table 1: Main operational sensors for ocean application.

Satellite	Sensor	Spectrum (μm)	Spatial resolution (m)	Temp. resol. (day)	Uses	Modelling
SeaStar	SeaWIFS	0.40-0.88	1300	1	Chlorophyll-a, Turbidity	Primary production
NOAA	AVHRR-2	3.5-12.55	1100	0.5	Brightness temperature	SST
Terra	MODIS	0.4-0.87	1000	1-2	Chlorophyll-a, Turbidity	Primary production
Terra	MODIS	3.66-12.27	1000	1-2	Brightness temperature	SST
Terra	ASTER	0.52-0.86	15	16	Coral reef, Turbidity	
Landsat	TM-5, 7	0.45-1.75	30	16	Coral reef, Turbidity	
IRS-P4	OCM	0.40-0.88	360×236	2	Chlorophyll-a, Turbidity	Primary production
Radarsat	Radarsat	5.6 cm	12.5-100	24	Sea ice, Oil spill, wave	
ERS	AMI	5.6 cm	12.5, 30	3	Sea ice, Oil spill, wave	
ERS	RA			3	Wave roughness	Wind direction, speed
QuickScan	SeaWind		25000	2	Wave roughness	Wind direction, speed

Applications in fisheries of remote sensing from manned orbital spacecrafts lie mostly in measuring characteristics of the physical and biological environment at the sea surface. The first application of satellite remote sensing in fisheries advisory in the US was in 1971 (Laurs 1993). This application has had a tremendous impact on the efficiency of American tuna fleets, often reducing search times by 25% to 40% (Simpson 1992). These technologies applied to fisheries still continue to expand and now include the Coastal Zone Color Scanner (CZCS), and the modern SeaWIFS satellites, which give a synoptic

view on the chlorophyll distribution in the oceans, and also the NOAA-AVHRR satellites which are used to map sea surface temperature in a short time. These oceanographic features can be successfully mapped in near real time using, for instance, Geographic Information Systems (GIS) tools.

To illustrate the wide range of applications of GIS and Remote Sensing in fisheries management, it is helpful to examine existing case studies. For example, combinations of satellite data sets have been used to identify correlations between ocean conditions and distribution of pelagic fish stocks such as albacore tuna and swordfish (Amidei 1983). From an operational perspective, Caddy and Carocci (1999) developed a GIS-based technique for monitoring interactions between fleets based at different ports, and their combined impacts on local resources. They extend the utility even further by using GIS for modelling the behaviour of these interactions. Freshwater systems can also benefit from GIS analysis. Salmonid populations in many countries are at risk due to the impacts of freshwater habitat fragmentation and degradation. These impacts can be identified and monitored using GIS technology.

The importance of GIS as an aid to spatial decision making has been increasingly recognised (Carver 1991), and recent developments in GIS have led to significant improvements in its capability to support decision-making processes (Jiang and Eastman 2000). GIS technology provides a computer-based system capable of integrating data, data storage, visualisation and management with data manipulation and analysis (Burrough and McDonnell 1998). On the other hand, Multi-Criteria Evaluation (MCE) is a GIS development, which facilitates decision support (Janssen and Rietveld 1990, Jankowski 1995). The MCE procedure employs weighted factors in a linear combination approach (Jiang and Eastman 2000), essentially integrating the evidence provided by each factor, which is believed to indicate a suitable site, by standardisation of each factor and then combining it using a weighted average. Criteria acting as constraints are simply classified as "1" for acceptable or "0" for unacceptable, and are used in the same way as for the Boolean logic approach (Eastman 1997).

In this research work, spatial distribution forecasting of capelin in the north of Iceland was performed using GIS and MCE in a Bayesian probabilistic framework. The MCE analysis evaluates a cartographic model to determine suitable areas for fishing, and then GIS selects areas that satisfy the highest potential. The model has been adapted from the ideas of Silva *et al.* (2000) and Mansor *et al*. (2001) who studied the associations of some pelagic species and chlorophyll *a* and SST obtained from remote sensing data and its uses to predict fishing ground areas according to a probabilistic statistical method. The probabilistic method used here is called the landslide index method (Westen 2001), which uses weights-of-evidence (Shafer 1976).

Errors are an inevitable component of all data, and their presence must be recognised and magnitude identified. This involves data quality measurements, as well as correctness, completeness, and integrity of spatial data (Chrisman 1991). Uncertainties require the use of statistical (probabilistic) analysis.

1.3 The species

Capelin (*Mallotus villosus*) is a small, silvery, pelagic schooling species and member of the family Osmeridae (McAllister 1964) and it is by far the most important pelagic fish stock in Icelandic waters (Vilhjálmsson 1983, 1984). In the Atlantic, capelin is abundant in the Barents Sea, around Iceland and Greenland, and off the Newfoundland and Labrador coasts. Vilhjálmsson (1994) gives a detailed description of global capelin distribution. Capelin has a key role in the food chain between animal plankton and fish. This species feeds on animal plankton in areas mainly far off the north coast, occasionally even beyond the Polar Front (Malmberg and Blindheim 1994). Around Iceland, juvenile capelin migrate to summer feeding grounds in the north where they grow rapidly, increasing their body weight by a factor of up to two, depending on age (Vilhjálmsson and Carscadden 2002). Most fish, but especially ground fish, feed on capelin at some stage in their life and it is estimated to be on average almost 50% by weight of the total food consumption of cod (*Gadus morhua*), which is the most important fish in Iceland. In the same way, capelin constitutes approximately 50% of the estimated total food ingested by Icelandic haddock (*Melanogrammus aeglefinus*) over the whole year. In Icelandic waters, the mean weights of cod aged 5-8 are positively correlated with capelin abundance (Vilhjámsson 2002).

When capelins grow and mature, their food requirements vary and items in their food spectrum change gradually (Panasenko 1984 and 1989, Aijad and Pushchaeva 1992, Skoldal *et al*. 1992). Therefore, capelin juveniles feed on nauplii of copepods and cyclopoids, and large, mature fish generally prey on adult copepods, euphausiids, and hyperiids, mainly in August, when their feeding concentrations in the western and central sectors of high latitude are broad. Abundance and distribution of plankton are therefore probably important links between the environment and abundance and growth of capelin (Jakobsson 1992). Growth of cod, however, seems not to be very dependent on hydrographical conditions, but more on abundance of capelin (Pálsson 1983, Malmberg 1986, Steinarsson and Stefánsson 1991) and other food.

Spawning takes place in late winter following migration towards the south and southwest coast of Iceland to ocean temperatures of 4-7° C (Vilhjámsson 2002), with a main peak in March. Capelin suffers mass mortality after spawning (Malmberg and Blindheim 1994). Maturing capelin (aged 2 and 3 years) usually undertake extensive northward feeding migrations into the Icelandic Sea and the Denmark Strait in spring and summer. The return migration takes place in September and October. By November, the adults have usually assembled near the shelf edge off northwest, north, and northeast Iceland.

Because of their ecological importance, and the large fishery (Gudmundsdóttir and Vilhjálmsson 2002, Vilhjálmsson and Carscadden 2002), intensive research on and monitoring of the state of the capelin stock in the Iceland-East Greenland–Jan Mayen area has been conducted since the late 1970s.

1.4 The capelin fishery in Icelandic waters

In addition to their key ecological role as a forage species, capelin is fished commercially. The abundance of capelin has initiated the development of large-scale commercial fisheries in the Barents Sea and the Iceland-East Greenland Area. Capelin in the Iceland-East Greenland-Jan Mayen area have been commercially fished since the mid-1960s, just after the collapse of the Norwegian spring-spawning herring stock in the late 1960s, when the pelagic fleets needed raw material to sustain themselves and the fishmeal plants. At first, the fishery was directed at pre-spawning and spawning concentrations in shallow coastal water west and south of Iceland in February and March, and yielded annual catches of 100 000-200 000 tonnes. In the early 1970s, the winter fishery expanded offshore east of Iceland in January, but declined rapidly in the late 1970s when recruitment of capelin was low. In the late 1970s, a summer capelin fishery began in deep water north of Iceland, based on the results of scouting surveys conducted by the Icelandic Marine Research Institute (MRI). Fishing is shared between Iceland, Norway, the Faeroe Islands and Greenland by special agreement but by far the largest quantities are fished by Iceland. Landings by the Icelandic fleet in the 2002 summer season were 180,000 tonnes and in the 2003 winter season 585,000 tonnes. On a calendar year basis, the landings by Icelandic vessels were 1,080,000 tonnes in 2002.

The fishery of capelin in the Iceland-East Greenland-Jan Mayen area has not changed much in the past 20 years with respect to fleet structure and fishing technology. It is predominantly pursued by purse seine during the summer and autumn and from January to March. The fishery targets the mature or maturing part of the stock, and therefore its location changes as the fish migrate. Maturing capelin aged 2 and 3 years usually undertake extensive feeding migrations northwards into the Icelandic Sea and the Denmark Strait in spring and summer, and the summer fishery is based on these migrations. During its first 15 years the summer/autumn fishery usually began in August, but since the mid-1990s the summer fishery has usually started about 1 month earlier. Nowadays, there is also an intensive winter fishery in shallow water off the south and west coast of Iceland. During years of good abundance, the winter capelin fishery may last throughout March and occasionally into the first week of April.

Extensive northward migrations cannot be described as annual occurrences. Figure 1, shows the geographic position of Icelandic catches of capelin (about 80-90% of the total catch) as tonnes per square nautical mile in the fishing seasons 1992/1993-2000/2001. Distribution of catches reveals large changes during the years 1992-2000, in terms of migrations and availability of capelin to the fishery in summer and autumn. There is a much greater regularity, both in landings and distribution, of winter catches than there is of the catch taken in summer and autumn of the years 1993-2001, the catching area being more or less continuous from off southeast Iceland to the central west coast (Vilhjámsson 2002). According to the catch distribution, it also seems that, during the feeding seasons of 1996 and 1997, the stock was distributed eastwards (east of the Kolbeinsey Ridge).

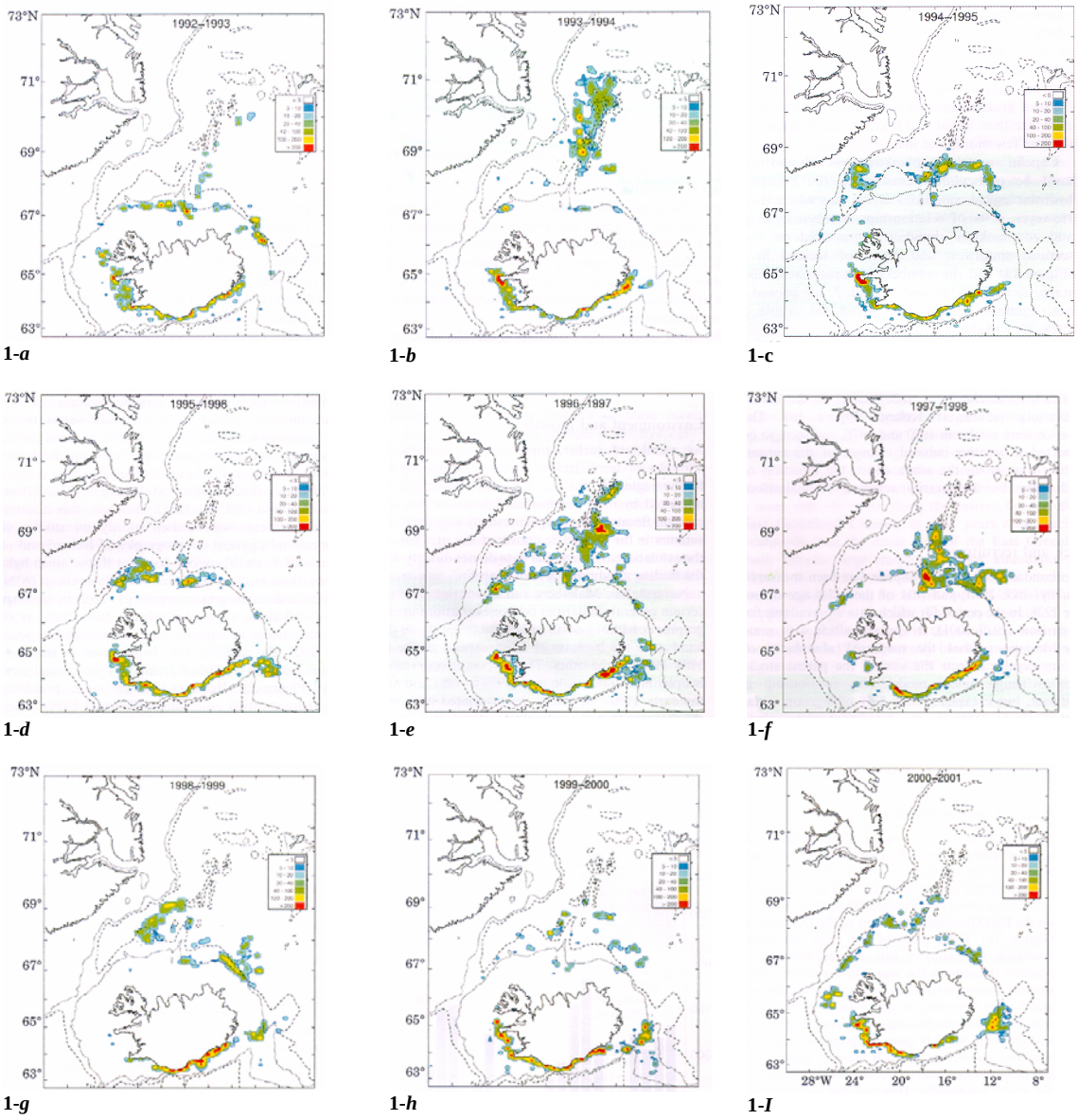

1-*a* **1-*b*** **1-c**

1-*d* **1-*e*** **1-*f***

1-*g* **1-*h*** **1-*I***

Figure 1: Icelandic catches of capelin in the Icelandic-East Greenland-Jan Mayen area in the 1992/1993-2000/2001 fishing seasons. Quantities are expressed in tonnes per square nautical mile. Catches north of 66° 30´N are from summer/autumn, and those south of 66° N between January and March (taken from Vilhjálmsson 2002).

According to Vilhjálmsson (2002), the most reasonable explanation of the different distribution patterns and variable success of the summer/autumn fishery in those years seem to be environmental variability.

Nowadays, the government of Iceland tries to develop these fisheries on sustainable bases by applying the Total Allowance Catches (TAC) that started in the summer of 2003. This is in line with scientific recommendations. The initial TAC for the 2003/2004 season that started in the summer of 2003 has been set at 360,000 tonnes pending further assessment during the coming winter.

1.5 The study area

The project was focused on the north Icelandic sea waters, between 65° 00' 00"- 69° 00´00" N and 10° 00' 00" – 25° 00' 00" W (Figure 2). This area has particular oceanographic conditions that influence the migration and distribution of capelin. Oceanographic structure and variability in this area depend on fluctuations in transports and properties in the major current systems in the region, i.e. the supply of warm water masses from the Irminger current, with temperatures ranging from 3-6°C, and cold waters from the East Greenland current that is generally colder than 0°C, while salinity is below 34.5 (Malmberg and Blindheim 1994).

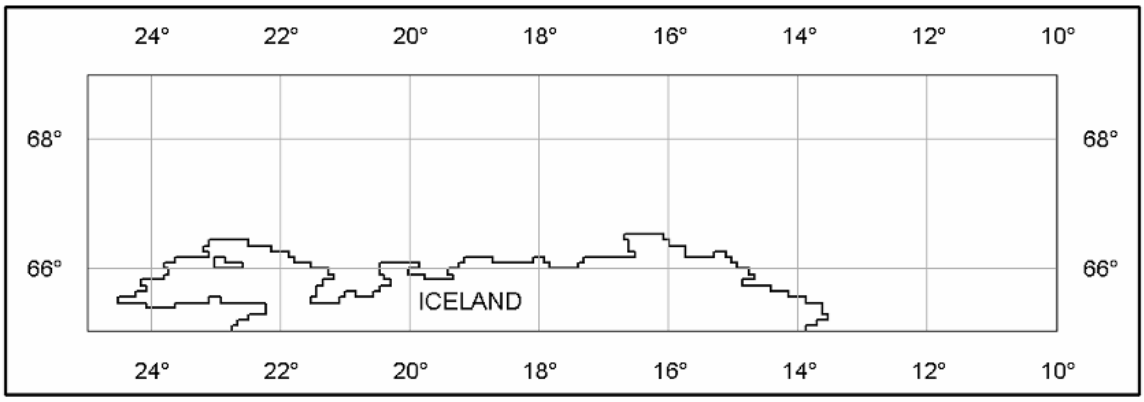

Figure : The study area.

The main features of the currents in the Iceland-East Greenland-Jan Mayen area are linked to bottom topography. Atlantic water of relatively high temperature and salinity predominates off the south and west coasts. Off the Vestfjord peninsula (northwest of Iceland), Atlantic water of the Irminger current flowing north just west of the Reykjanes Ridge splits into two branches. The larger branch flows west towards Greenland, while the smaller, the North Icelandic Irminger current, flows eastwards onto the shelf north and, to some extent east of Iceland. A coastal current, essentially driven by gravitational forces resulting from land run-off, runs in a clockwise direction around Iceland.

Conditions in the waters of the Icelandic sea are considerably milder. Variations in the relative strength of these ocean currents have resulted in large changes in the hydrography of north Icelandic waters, and probably also in the Icelandic sea further north (-1 to 2 °C in the East Greenland and East Icelandic currents). On the other hand, the hydrography of the Atlantic water south and west of Iceland is more stable. The hydrographical conditions in Icelandic waters in 2000 revealed in general relatively high temperatures and salinities as in the last 2-3 previous years. The salinity in the warm water from the south was higher than has been observed over the last decades, and these conditions have been evident since 1997. This was further evidence of the Atlantic inflow into North Icelandic waters (ICES 2000), and provides an important source of nutrients to the sea north of Iceland. Because of its relatively high nutrient concentration and the efficiency in the surface layer by eddy diffusion are better than the highly stratified Arctic

or polar waters. This makes for a longer-lasting period of phytoplankton production and richer stocks of zooplankton during warm periods than during cold ones (Thórdardóttir 1984, Stefánsson and Ólafsson 1991, Astthórsson and Gíslason 1998).

In a polar regime, conditions for plankton production are different. Here there is a surface layer with low density and relatively strong density gradients before the warming in the spring starts. The warming results in a shadow surface layer with a short and intense spring bloom (Thórdardottir 1977, Stefánsson and Ólafsson 1992). The nutrients are quickly depleted because of the sharp pycnocline below the mixed layer. Blooming later in the summer seems to be almost negligible. In North Icelandic waters the decrease in abundance of zooplankton is considerable (Astthórsson *et al.* 1983). Also low temperatures as such may be an important factor. Adult cod avoids low temperatures and seldom occurs in abundance in temperatures near 0°C. Although it is claimed that cod larvae and juveniles adapt better to low temperatures than adult fish (Goddard *et al*. 1992) and it has an adverse impact on the recruitment.

1.6 The rationale for the project

The present work is intended to address the most important issues including:

-Economic impact: The determination of probable fishing areas, allows minimising the searching time and the operational cost of the vessels (Nieto 1999). Consequently, CPUE can be increased and profit can be improved.

-Ecologic impact: Better planning allows for planning and diminishing of the impact to the stock. Capelin is a schooling fish and very sensitive to collapse, a phenomenon that is not surprising for a species with such a high mortality rate and short life. Government and private fishing companies can plan for the optimal management of the fishery based on ecological considerations.

-Social impact: Government and decision-makers can use this as a tool in the decision making process for planning fisheries activities on a sustainable basis. This includes the participation of stakeholders such as fisherman, private sector and government.

-Migrating: This methodology can be transferred to pelagic fisheries in Mexico, by incorporating the local environmental variables and fish biology.

1.7 The approach

Spatial and temporal modelling includes remote sensing techniques, GIS, Bayesian theory (probability functions), fuzzy logic (possibility functions) and MCE methods.

1.8 The state of the art

Fish forecasting has been studied in many countries around the world. This includes non-scientific forecasting (some of which involve environmental input in some way), as well

as scientific and the use of advanced technologies (for instance remote sensing from manned orbital spacecraft and GIS tools). Buoys, satellites, and other RS technologies produce information on a large geographic scale. Satellite systems such as the Advanced Very High Resolution Radiometer (AVHRR) and Coastal Zone Colour Scanner (CZCS) have produced data regarding ocean surface temperature and colour (chlorophyll distribution), respectively (Amidei 1983).

More recently, satellites carrying the Sea-viewing Wide Field of View Sensor (SeaWiFS) and Moderate Resolution Imaging Spectroradiometer (MODIS) have dramatically improved the spectral and spatial resolution of available imagery (Simpson 1994). Based on these technologies, numerous fisheries applications for these data sets have been implemented or proposed for development purposes. Several countries have already incorporated fisheries data into GIS-based management plans (Simpson 1992).

Temperatures of water or air are frequently used in studies of climate change on fish abundance and distribution (Austin 1978). Early attempts at scientific prediction of fish abundance using environmental input data included Walford's (1938) efforts to relate the distribution of haddock eggs on George Bank to the density structure of the water. Later studies at the Sandy Hook Marine laboratory in 1964 indicated that the annual spring influx of warm season fisheries into the Mid-Atlantic coastal area is controlled by temperature conditions for such species as bluefish, striped bass and mackerel. This study showed that the large schools of migrating mackerel observed are restricted within a narrow temperature zone at 48 to 56 °F.

Modern methodologies such as GIS and Multi-Criteria Evaluation have also contributed to improving the decision making process in fisheries. This is well represented by the work of Mansor *et al*. (2001), who has developed a satellite fish forecasting system in the South China Sea based on Remote Sensing, GIS and Multi-Criteria Evaluation techniques. The final result was a DSS software tool (TroFFS) for fish forecasting process in tropical waters.

O'Brien *et al.* (1974) developed a forecast capability for Coho salmon off Oregon, by establishing a relation between the location of Coho salmon and the position and state of the coastal upwelling front, which in turn were related to the surface wind field. By using a rapid information dissemination system, they were able to predict fishing conditions on a daily basis, enabling fishermen to increase their yield per unit effort.

Regarding temperature and fishing catches, the report of the Matahari expedition (1996), carried out off the coast of Peninsular Malaysia, shows high correlation between historical catches of pelagic fish and the warm waterfront in that area.

Silva *et al*. (2000), explored the relationship of jack mackerel (*Trachurus murphyi*), anchovy (*Engraulis ringens*) and sardine (*Sardinops sagax*) catches in the north of Chile, related with SST and chlorophyll parameters obtained from remote sensing. They concluded that anchovy is found in the frontal zone of the upwelling regions and is associated with higher chlorophyll values than the others species. Similar research was

carried out by Barbieri *et al.* (1990), in the evaluation of the potential swordfish (*Xiphias gladius*) fishing grounds of central Chile, by the use of remote sensed sea surface temperature satellite data and Geographic Information Systems. They considered as input variables influencing the distribution of swordfish such as sea surface temperature and thermal gradient. Furthermore, they concluded that the analysis of historical records of these environmental parameters in the fishing areas would allow predicting fishing grounds.

Perez-Marrero (2001) studied the sea surface thermal conditions in the North Atlantic (Northwest African Coast) in relation to fishery activities using SST extracted from AVHRR of the NOAA series satellite, for the period 1985-1994, finding that SST field had some relationship with tuna fisheries activities in these areas.

Caddy and Carocci 1999 used GIS techniques and a Gaussian Effort Allocation Model to describe the spatial allocation of fishing intensity from coastal ports with an example of application in Digby Bay (Nova Scotia). In their work, they introduce the concept of "friction of distance", which involves cost, in order to calculate the shortest distance for each port of origin to each point on the fishing grounds.

Based on satellite technologies, Triñanes *et al.* (2002) used the simple processing techniques of Remotely Sensed Images on pelagic fisheries in the Gulf of Biscay of the North East Atlantic. The remote sensed data included NOAA/AVHRR and SeaWIFS images. By using RS techniques, they could detect possible fishing areas associated with frontal zones which it likely to be of interest to pelagic fishers. Similarly, Zheng, *et al.* (2002), describes spatial relationships between whiting, *Merlangius merlangus* (Linnaeus 1758), abundance in the northern North Sea and contemporaneous measures of environmental conditions: sea surface temperature, sea bottom temperature, and depth, in a GIS environment and Generalised Additive Models (GAMs), which where used to provide quantitative descriptions of the relationships between local abundance and environmental conditions.

Optical sensors are not the only ones used to study the fisheries' activities. A microwave sensor such as Synthetic Aperture Radar (SAR) has capabilities to get data through cloudy regions, especially in high latitude areas, and canopy. The study of Clemente *et al*. (2002), describes the use of Spaceborne Synthetic Aperture Radar in the monitoring and management of the herring roe fisheries region Togiak Bay, Alaska, by using images from RADARSAT-1 satellite SAR and ERS-1 and ERS-2. With the use of these images, they could detect areas of high biological productivity, which is associated with phytoplankton blooms, as an indicator of better fishing conditions.

1.9 The objectives

1.9.1 General objective

To predict the potential fishing grounds of the small pelagic fish capelin (*Mallotus villosus*) in the north Icelandic sea waters.

1.9.2 Specific objectives

To perform a MCE to locate areas with high potential for pelagic fisheries in Iceland, using Geographic Information Systems and Remote Sensing techniques.

To propose a standard methodology that can be applied by government and stakeholders involved in the fisheries' activities.

1.10 The research questions

- What is the potential of the pelagic fisheries in the north Icelandic sea waters based on historical fishing ground information, Sea Surface Temperature (SST) and productivity (Chlorophyll *a*)?

- Among these areas, where are the sites with the highest potential for fishing and how many areas are available?

- How does the highest potential area respond to the uncertainty in the input data (sensitivity analysis)?

1.11 The goals

1- To explore the association between the small pelagic fish capelin (*Mallotus villosus*) and SeaWIFS chlorophyll and NOAA-AVHRR SST.

2- To develop GIS-based and Multi-Criteria Evaluation (MCE) models to forecast the potential fishing grounds in the north of Iceland using knowledge-driven (expert, Fuzzy logic functions) and data-driven (Bayesian probabilistic theory) approaches.

2 THEORICAL BACKGROUND

2.1 Remote sensing fundaments

Remote sensing is the science (and to some extent, art) of acquiring information about the Earth's surface without actually being in contact with it. This is done by sensing and recording reflected or emitted energy and processing, analysing, and applying that information (Curran 1985). The main elements of a remote sensing system are described in Figure 3. These seven elements comprise the remote sensing process from beginning to end.

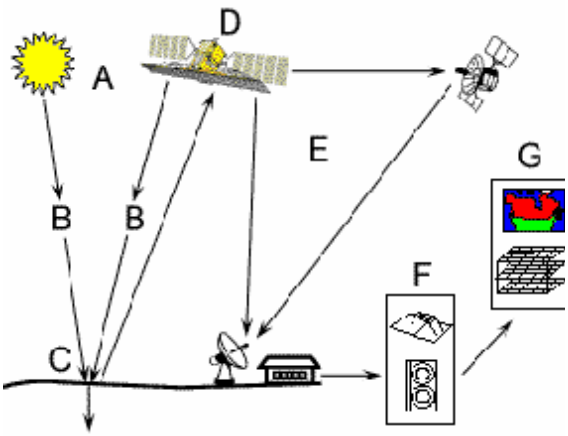

A: Energy source or illumination
B: Radiation and the atmosphere
C: Interaction with the target
D: Recording of energy by the sensor
E: Transmission, reception, and processing
F: Interpretation and analysis
G: Application

Figure 2: The remote sensing basis and process.

2.1.1 Sea surface temperature algorithms

In the nadir measurements in cloudless regions the sea surface temperature, T_s should be of the form:

$$Ts = a_0 T_i + a_1 (T_i - T_j) + a_2 \qquad (1)$$

Where T_i and T_j are the brightness temperatures determined from the radiance values in two different infrared window channels ***i*** and ***j***. The constant a_0 is close to 1 suggesting that the infrared temperature measured in any one of these channels is close to the sea surface temperature. The temperature difference term makes a small correction to this temperature for atmospheric transmittance. The term a_2 is a small correction factor associated with the different atmospheric brightness temperatures at different channels.

Based on empirical comparisons of AVHRR data and buoy measurements, McClain *et al.* (1985), and Bernstein (1982), found two sets of algorithms for combining the radiance measurements at the three emitted infrared window channels - one set for night time and one set for daytime. The algorithms used at night can employ the $T_{3.7}$channel. For daytime algorithms, the $T_{3.7}$ channel contains reflected skylight and only combinations of T_{11} and T_{12} are useful.

In general there are three classes of sea surface temperature algorithms. The "split-window" algorithm uses the T_{11} brightness temperature as the lowest order estimate of sea surface temperature and the difference $T_{11} - T_{12}$ to correct for the atmosphere. The "dual-window" algorithm uses the T_{11} brightness and the difference $T_{3.7} - T_{11}$ to correct for the atmosphere. Finally, the "triple-window"" algorithm uses the T_{11} brightness and the difference $T_{3.7} - T_{12}$ to correct for the atmosphere. In addition, there are corrections terms that must be applied to adjust the measurements made of nadir. If we define θ to be the sensor zenith angle, then the three algorithms have the form:

Split $(mc)_1$ $\quad Ts = A_0 T_{11} + A_1 (T_{11} - T_{12}) + A_2 (T_{11} - T_{12}) (\sec\theta - 1) + A_3 \sec\theta + A_4 \qquad (2)$

Dual $(bz)_1$ $Ts = A_0T_{11}+A_1 (T_{3.7}–T_{11}) +A_2(T_{3.7}–T_{11}) (sec\theta–1)+A_3sec\ \theta + A_4$ (3)

Triple $(tw)_1$ $Ts = A_0T_{11}+A_1(T_{3.7}–T_{12})+A_2(T_{3.7}–T_{12})(sec\theta–1)+A_3sec\ \theta + A_4$ (4)

The temperatures can either be in degrees Celsius or Kelvin. Appendix I describes the coefficients employed to compute sea surface temperature given these functional forms using both the Celsius and Kelvin temperature scales.

2.1.2 Principles of operation of the sensor AVHRR

The AVHRR is a four- or five-channel scanning radiometer that detects emitted and reflected radiation from Earth in the visible, near-, middle-, and thermal-infrared regions of the electromagnetic spectrum. A fifth channel was added to the follow-on instrument designated AVHRR/2 and flown on NOAA-7, -9, -11, and -14 to improve the correction for atmospheric water vapour. The AVHRR is a cross-track scanning system. The IFOV of each sensor is approximately 1.4 milliradians, giving a resolution of 1.1 km at the satellite sub-point. There is about a 36 percent overlap between IFOVs (1.362 samples per IFOV). The scanning rate of the AVHRR is six scans per second, and each scan spans an angle of +/- 55.4 degrees from the nadir. The NOAA satellites orbit Earth at an altitude of 833 km. From this space platform, the data are transmitted to a ground receiving station. Launch and available dates for the TIROS-N series of satellites from CCRS are showed in Table 2. In addition, Table 3 shows the primary use of each channel and spectral regions and bandwidths on the respective NOAA platforms.

The AVHRR can operate in both real-time and recorded modes. Direct readout data are transmitting to ground stations of the automatic picture transmission (APT) class at low resolution (4 km x 4 km) and to ground stations of the high-resolution picture transmission (HRPT) class at high resolution (1 km x 1 km).

Table 2: Satellite launches history for the TIROS-N series.

Satellite	**Launch date**	**Date range.**
TIROS-N	13-Oct-1978	19-Oct-1978 to 30-Jan-1980
NOAA-6	27-Jun-1979	21-Aug-1984 to 23-Jan-1986
NOAA-B	29-May-1980	Failed to achieve orbit
NOAA-7	23-Jun-1981	24-Jul-1983 to 30-Dec-1984
NOAA-8	28-Mar-1983	24-Jul-1983 to 13-Aug-1985
NOAA-9	12-Dec-1984	16-Sep-1985 to 19-Mar-1995
NOAA-10	17-Sep-1986	11-Oct-1986 to 15-Nov-1993
NOAA-11	24-Sep-1988	28-Jun-1989 to 13-Sep-1994
NOAA-12	14-May-1991	11-Aug-1993 to present
NOAA-14	30-Dec-1994	15-May-1995 to present
NOAA-15	1998	to present
NOAA-16	2001	to present

Table 3: Spectral features and uses of NOAA-AVHRR sensor.

Channel	Wavelength [µm]	Primary use
1	0.57 – 0.69	Daytime Cloud and Surface Mapping
2	0.72 – 0.98	Surface Water Delineation, Vegetation Cover
3	3.52 – 3.95	Sea Surface Temperature, Nighttimes Cloud Mapping
4	10.3 – 11.40	Surface Temperature, Day/Night Cloud Mapping
5	11.4 – 12.40	Surface Temperature

2.1.3 A brief description of ocean colour measurements

When visible light from the sun illuminates the ocean surface, it is subject to several optical effects. Foremost among these effects are light reflection and absorption. Reflection beneath the water surface is generally inefficient, returning only a small percentage of the light intensity falling on the ocean surface. Absorption selectively removes some wavelengths of light while allowing the transmission of other wavelengths.

In the ocean, light reflects ofa particular matter suspended in the water, and absorption is primarily due to the photosynthetic pigments (chlorophyll) present in phytoplankton. The net result of these optical interactions is light radiating from the ocean surface, the "water-leaving radiance". Radiometers are instruments that measure the radiance intensity at a given wavelength of light. The measured radiance may then be quantitatively related to various constituents in the water column that interact with visible light, such as chlorophyll. The concentration of chlorophyll, in turn, may be used to calculate the amount of carbon being produced by photosynthesis, which is termed primary productivity (SeaWIFS 2003).

Chlorophyll-*a*, is present in all oxygenic photo synthesizers, and as such is used to monitor phytoplankton in aquatic environments, characterised by well-defined and specific optical properties in the visible range. chlorophyll is suitable for direct observation with optical instruments (Iluz 2003).

2.1.4 SeaWiFS OC4 Chlorophyll extraction algorithm

Several algorithms exist for the retrieval of the chlorophyll concentration in sea waters, since the CZCS satellite and its successor the SeaWiFS satellite were launched. Appendix II shows empirical algorithms to extract chlorophyll concentration developed by several authors. A basic algorithm used to determine the chlorophyll concentration is based on the ratio of radiance or reflectance measured in the blue and green spectral bands (O'Reilly *et al*. 1998). A polynomial is usually used to represent the relation between the algorithm of the band ratios and the logarithm of chlorophyll concentration. The coefficients of the polynomial are found by regression between the band ratios and the sea-truth value of chlorophyll concentration measured from water samples taken at various places.

The newest OC4 algorithm (SeaWIFS project) has been tested to improve the capabilities to detect the variations on chlorophyll concentration in the different areas of the oceans.

O'Reilly *et al*. (2000), provided a summary of how the OC4 chlorophyll algorithm works. OC4 is a 'maximum band ratio' algorithm where the maximum of three band ratios (443/555, 490/555, and 510/555) is used to predict chlorophyll concentration as follow:

$$\text{chlorophyll-}a \text{ (mg/m3)} = 10.0^{\wedge} (0.405-2.900\mathbf{R}+1.690\mathbf{R}^2+0.530\mathbf{R}^3-1.144\mathbf{R}^4) \quad (5)$$

Where: $\mathbf{R}= \log10 (Rrs_{443/565}>Rrs_{490/565}>Rrs_{520/565})$ (6)

Over most of the deep ocean, chlorophyll concentrations are below 0.3 mg m-3, and water-leaving radiance in the 443nm band exceeds the radiance in the 490nm and 510nm bands. At chlorophyll concentrations above 0.3 mg m-3 and below 1.5 mg m-3 (values typically found on continental shelves), water-leaving radiance in the 490nm band is usually greater than the values for the 443 and 510nm bands. Finally, at chlorophyll concentrations above approximately 1.5 (mg m-3), frequently found near shore, water-leaving radiance in the 510nm band exceeds that measured in the 443nm and 490nm bands. In fact, in both chlorophyll-rich waters and phytoplankton blooms, the estimate of water-leaving radiance for the 443nm band (after atmospheric correction) may be noisy and too low to make accurate chlorophyll estimates. The OC4 algorithm takes advantage of the natural shift in the dominant radiance band, and by using the brightest band (443,490,510) in the band ratio, the algorithm is able to estimate chlorophyll concentrations with a high level of accuracy over the wide range that exists in the global ocean.

2.1.5 Principles of operation of the sensor SeaWIFS

The first instrument to collect scientific data on the colour of the ocean was the Coastal Zone Colour Scanner (CZCS), an instrument on the NIMBUS-7 satellite, which operated from November 1978 to June 1986. The operational parameters of the SeaWiFS mission were based on the heritage of the CZCS mission and were designed to improve the acquisition and accuracy of ocean colour data for global and regional study of ocean biology and related physical oceanographic phenomena.

SeaWiFS is a spectroradiometer, which means that it measures radiance in specific bands of the visible light spectrum. The advantage of observing the oceans with a space-based spectroradiometer is the global coverage that a satellite provides. The disadvantage is that interfering optical effects, primarily light scattering in the atmosphere, must be accounted for to provide an accurate measurement of the water-leaving radiance.

SeaWiFS was launched August 1, 1997 by a Pegasus XL launch vehicle. Data acquisition commenced on September 4, 1997. SeaWiFS scanned approximately 90% of the ocean surface every two days. All of the data products are stored in the Hierarchical Data Format (HDF), which was developed by the National Centre for Supercomputing Applications (NCSA) at the University of Illinois. Nominal orbit parameters for the OrbView-2 satellite and SeaWIFS sensor are showed in Table 4 through Table 6.

Table 4: Nominal orbit parameters for the OrbView-2 satellite.

Orbit	Sun-synchronous
Nominal altitude	705 km
Equator Crossing	Noon +/- 20 min., descending node
Inclination	98 deg 12 min
Orbital Period	98.9 min

Table 5: Nominal orbit parameters for SeaWiFS.

Parameter.	Features.
Scan Width	58.3 deg (LAC); 45.0 deg (GAC)
Scan Coverage	2,800 km (LAC); 1,500 km (GAC)
Pixels along Scan	1,285 (LAC); 248 (GAC)
Nadir Resolution	1.13 km (LAC); 4.5 km (GAC)
Scan Period	0.167 seconds
Tilt	-20, 0, +20 deg
Digitisation	10 bits

Table 6: Nominal radiometric parameters for SeaWiFS.

Band	Centre wavelength (nm)	Primary use
1	412 (violet)	Dissolved organic matter (incl. gelbstoffe)
2	443 (blue)	Chlorophyll absorption
3	490 (blue-green)	Pigment absorption (Case 2), K(490)
4	510 (blue-green)	Chlorophyll absorption
5	555 (green)	Pigments, optical properties, sediments
6	670 (red)	Atmospheric correction (CZCS heritage)
7	765 (near IR)	Atmospheric correction, aerosol radiance
8	865 (near IR)	Atmospheric correction, aerosol radiance

2.2 Geographic Information Systems

Geographic Information System (GIS) can be defined as a computer assisted system for acquisition, storage, analysis and display of geographic data (Zhou 1995). Burrough and McDonnell (1986), define a GIS as a computer based system that enables capture, modelling, manipulation, analysis and presentation of geographically referenced data (Figure 4). For many years, this has been done using analogues data sources, manual processing and the production of paper maps. The introduction of modern technologies has led to an increased use of computers and digital information in all aspects of spatial data handling (Zhou 1995).

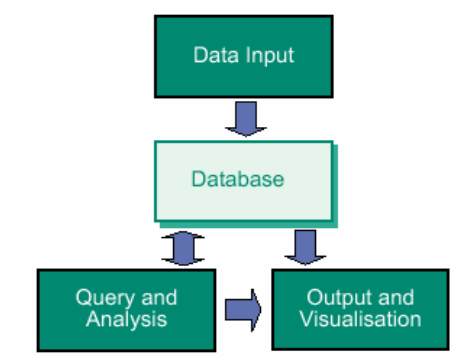

Figure 3: Functionality of a GIS database.

Any GIS makes use of geographical and attribute data that are associated for displaying and making queries. Geographical data are very often recognised and described in terms of well established geographical "object" of phenomena. These data are referenced to locations on the earth's surface by using a standard system of coordinates.

2.3 Multi Criteria Evaluation

The primary issue in Multi-Criteria Evaluation (MCE) is concerned with how to combine the information from several criteria to form a single index of evaluation. Criteria are divided into factors and constraints. Factors are defined as spatial features, which influence the suitability of a spatial unit for the given objective (e.g., for non point pollution). Constraints then are areas, which have no suitability. With a weighted linear combination, continuous factors are combined by applying a weight to each according to its relative importance and followed by a summation of the results to yield a suitability map. In some analysis, especially those concerning data from different measurement unit and coming from different sources need to be standardised. Based on these principles, constraint maps must be binary (0=not suitable, 1=suitable) and the factors maps must be also standardised to a common range of values (e.g., 0-1 in a Fuzzy set, 0-255 as an image range), because of different scales upon which they are measured. Thus each factor will have an equivalent measurement basis before any weights are applied (Voog 1983).

2.4 Integration of GIS and MCE

GIS and DSS can play an important role in land use planning and site selection where the main task and objective is to give the answer to the questions about "Where are the best sites for…?", "How many areas are available for…?". Potential site selection for any activity is typically a decision matter where several alternatives have to be analysed and finally the best one retained. In this way MCE fits very well with this type of situation and can help to select the best solution by evaluating several criteria and alternatives. GIS is one of the best technologies to handle spatial data and to provide the suitability of the area according to several criteria involved in the problem. Therefore GIS is used for

spatial data preparation and for visualisation; both important aspects of spatial decision-making.

The most common procedure used to integrates GIS and MCE for suitability analysis is the weighted linear combination (Voogd 1983, Eastman 1997). With a weighted linear combination, factors are combined by applying a weight to each followed by a summation of the results to yield a suitability map, i.e.:

$$S = \sum_i w_i x_i \qquad (7)$$

Where *S* is the composite suitability score, based on individual scores *x* and their weights *w*, which usually sum to 1. If Boolean (yes/no) factors are also included, these multiply the suitability score, to eliminate those without all 'true' scores for the Boolean factors *c*:

$$S = \sum_i w_i x_i \cdot \prod_j c_j \qquad (8)$$

According to this, the best sites are selected based on the highest scores (Tomlin 1991).

2.5 Assigning weights to the criteria

2.5.1 Knowledge- driven models

Different criteria usually have different levels of importance, for example the criterion "sea surface temperature" can be much more important for predict potential fishing ground in pelagic fishes than "chlorophyll-*a* concentration" or "historical record of CPUE relative abundance". It is therefore necessary to incorporate some form of criteria weighting to take care of their relative importance. There are many methods to obtain weights for the factors. Weights can be obtained by subjective or probabilistic way (Table 7). These are called as "knowledge driven" and "data driven" methods, respectively. Criteria weighting was done in this research using both methods. The first approach is concerned with the subject of a decision maker and is thus subjective. The most common method used to obtain weights based on decision maker preferences is based on the technique devised by Saaty (1977), which compares each factor in pairs until a self-consistent set of weights is found. The expert assigns an importance to each criterion, as show in Figure.5:

extremely	*ery*	*strongly*	*moderately*	*equally*	*moderately*	*strongly*	*very*	*extremely*
1/9	1/7	1/5	1/3	1	3	5	7	9

less important ←========== → *more important*

Figure 4: Scale of preferences to assign scores, based on Saaty (1977).

Now with the criteria on a common scale, and weighted, we can compute overall suitability with MCE.

Table 7: Suitability models, divided into data-driven and knowledge-driven models (taken from Bonham-Carter 1998).

Type	Model parameters	Example
Data-driven	Calculated from training data	Logistic regression Weights of evidence Neural network
Knowledge-driven	Estimated by an expert	Fuzzy logic Dempster-Shafer belief theory

The second method (data driven) uses a Bayesian probabilistic approach. The theory and development of the method is described below.

2.5.2 Bayesian method

The Bayesian approach to the problem of combining datasets uses a probability framework. Boolean, Index Overlay, Fuzzy logic models are subjective empirical models, with the rules, weights or Fuzzy membership values being assigned subjectively, using a knowledge of the process involved to estimate the relative importance of input data layers.

The Bayesian model assigns the weighting of individual data layers based on a Bayesian probability model. It introduced the idea of prior and posterior (conditional) probability. The prior probability can be successively updated with addition of new evidence, so that the posterior probability from adding one piece of evidence can be treated as the prior for adding a new piece of evidence (Bonham-Carter 1998).

According to the Bayesian probability theory, the favourability for finding the element D, given the presence of the evidence can be expressed by the conditional probability:

$$P\{D/B\} = \frac{P\{D \cap B\}}{P\{B\}} \qquad (9)$$

where $P\{D/B\}$ is the conditional probability of D given the presence of a binary pattern. The *posterior* probability in terms of *prior* probability satisfying the relationship:

$$P\{D/B\} = P\{D\}\frac{P\{B/D\}}{P\{B\}} \qquad (10)$$

A similar expression can be derived for the posterior probability of an event occurring given the absence of an indicator anomaly pattern. Thus:

$$P\left\{D/\overline{B}\right\} = P\{D\}\frac{P\left\{\overline{B}/D\right\}}{P\left\{\overline{B}\right\}} \qquad (11)$$

2.6 Odds formulation

The same model can be expressed in an odds form. Odds are defined as a ratio of the probability than an event will occur to the probability that it will not occur. The weights of evidence method use the natural logarithm of odds, known as log odds or **logits**. The expression can be converted to:

$$\frac{P\{D/B\}}{P\left\{D/\bar{B}\right\}} = \frac{P\{D\}P\{B/D\}}{P\left\{D/\bar{B}\right\}P\{B\}} \qquad (12)$$

By adding the conditional probability, leads the desired expression:

$$O\{D/B\} = O\{D\}\frac{P\{B/D\}}{P\left\{\bar{B}\right\}} \qquad (13)$$

Where $O\{D/B\}$, is the conditional (*posterior*) odds of D given B, $O\{D\}$ is the *prior* odds of D and $P\{B/D\}/P\left\{B/\bar{D}\right\}$ is known as the **sufficiency ratio, LS**. In weights of evidence, the natural logarithms of both sides of the equation (13) are taken, and $\log_e$ LS is the positive weight of evidence $\mathbf{W}^+$, which is calculated from the data. Then:

$$\log it\{D/B\} = \log it\{D\} + W^+ \qquad (14)$$

A similar algebraic manipulation leads to the derivation of an odds expression for the conditional probability of D given the absence of the binary indicator pattern, with the result being:

$$O\left\{D/\bar{B}\right\} = O\{D\}\frac{P\left\{\bar{B}/D\right\}}{P\left\{\bar{B}/\bar{D}\right\}} \qquad (15)$$

The term $P\left\{\bar{B}/D\right\}/P\left\{\bar{B}/\bar{D}\right\}$ is called the **necessity ratio, LN**. In weights of evidence, $\mathbf{W}^-$ is the natural logarithm of LN, or $\log_e$ LN. Thus in logit form, Equation (15) is:

$$\log it\left\{D/\bar{B}\right\} = \log it\{D\} + W^- \qquad (16)$$

LS and LN are also called **likelihood ratios**. In addition to this, it is important to point out that:

1. The value of LS id greater than 1, whereas LN is in the range (0, 1). This indicates that the presence of the binary pattern, B, is important positive evidence to find D. However, if the pattern is negatively correlated with D, LN would be greater than 1 and LS would be in the range (0.1). If the pattern is uncorrelated with the deposits, then LS=LN=1, and the *posterior* probability would equal the *prior* probability, and the probability of D would be unaffected by the presence or absence of the binary pattern.

2. Similarly, W^+ is positive, and W^- is negative, due to the positive correlation between the points and the binary pattern. Conversely W^+ would be negative and W^- positive for the case where fewer points occur on the pattern than would be expected due to chance. If D is independent of whether the pattern is present or not, then $W^+ = W^- = 0$, and posterior equals the prior, as above.

3. The values of the posterior probability calculated using weights or the likelihood ratios are identical to those calculated directly using the conditional probability equations.

3 METHODOLOGY

The methodology includes several sections, which correspond to different stages of the project. The first section describes the data used including the source, and spatial and temporal resolution. These data were transformed to ILWIS (GIS) format to create factor maps using a standard grid of 9 km by 9 km cell size, and then combined according to the cartographic model (Figure 6). The following sections include the validation of SeaWiFS chlorophyll *a* concentration (Chl) and NOAA-AVHRR Sea Surface Temperature (SST) remote sensed data with *in-situ* historical database, and the implementation of a GIS-based fishing ground forecasting model. The fishing ground forecasting model included Chl and SST remote sensed information from July 16, 2003. Multi-Criteria Evaluation (MCE) techniques and constraints maps (Boolean maps, which includes clouds and land coverage) were applied to identify the most suitable sites for pelagic fish capelin, based on the historical CPUE data and its association with the available physical and biological parameters. Fuzzy logic operators were used in order to enhance evidences to forecast the spatial distribution of capelin. Final probability maps were split into three different categories (e.g. “High”, “Medium” and “Low” probability), and then quantified in terms of area. Weights of the factor maps were changed, representing the relative importance of each factor map in the MCE problem. The entire approach can be viewed following sections below.

3.1 The conceptual model

Figure 6, shows the conceptual model implemented to predict pelagic fishing grounds in the north Icelandic waters.

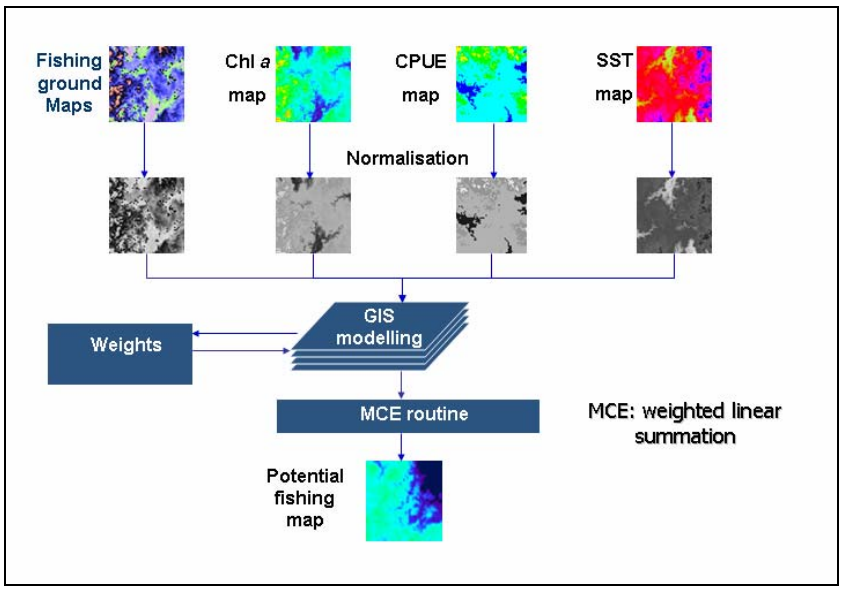

Figure 5 : Conceptual model to predict capelin fishing grounds in the north Icelandic waters. RS, GIS and MCE technologies are involved overall the process.

The model is simple, using only two input parameters (e.g. SST and Chl remote sensed data), which are assumed to be the most important physical and biological parameters, respectively, that influence the spatial distribution of capelin. Additional information as historical fishing ground areas and CPUE abundance maps can be added in order to improve the results obtained. In spite of the simplicity of the model, this involves GIS and image processing techniques combined in a MCE procedure.

3.2 Data acquisition

3.2.1 Fisheries data

Catch-per-unit-of-fishing-effort (CPUE) data were obtained from the Marine Research Institute (MRI) in Iceland. A total of 17,144 records corresponding to the summer season capelin catches, from August 1992 to July 2003, were analysed and transformed to ILWIS format. The database included date, geographic position (Lat-Lon), and catch. Frequency and total catches per day in May were converted to point maps and overlaid with Chl and SST remote sensed images corresponding to the same day.

3.2.2 Satellite data

NOAA-14 and NOAA-16 AVHRR-LAC HRPT Level 1b images were acquired from the NERC Satellite Receiving Station at the University of Dundee. These images were used to validate SST with *in-situ* information and also in the fishing ground forecasting model. The search period for images was from late May 1998 (when SeaWiFS just started to operate) to 2003. Only images from May 22 2000, May 23 2001, and July 16 2003, were selected to validate the SST values, and for the fishing ground forecasting model implementation, respectively. Most images were cloud contaminated in the period corresponding to *in- situ* data. The SST HRPT images were displayed using HRPT reader software. SST and geographic position values were obtained directly from the L1b images. The original SST information was obtained using a Multi-Channel Algorithm (McClain, *et al*. 1985) (see section 2.2.1, and Appendix I). A subset of these images was obtained for the study area (Table 8) and re-sampled in a standard projection using a least-squares transformation equation and the nearest neighbour resembling technique (Lillesand and Kiefer 2000). The output grids of 0° 5' 16.406" (9 km x 9 km) represent a SST matrix data of 46 lines and 171 columns.

Table 8 : Matrix of extreme coordinates for the area used for a subset of images.

	LONGITUDE	**LATITUDE**
MINIMUM	-25° 00'	65° 00'
MAXIMUM	-10° 00'	69°00'

SeaWiFS Chl images.

SeaWiFS Chl images corresponding to the same period of NOAA-AVHRR images were accessed and ordered using the Goddard DAAC's SeaWIFS data browser in a Level 3-GAC gridded data. Images was searched by using Quick look database in the same data browser, and obtained by File Transfer Protocol (FTP). The original grid of the L3 GAC images is 0° 5' 16.406" (9 km x 9 km). Subsets of these images were obtained using the extreme coordinates showed in Table 8, to represent a Chl matrix data of 46 lines and 171 columns. The Chl concentrations were obtained using the CZCS-type formula:

Chlorophyll *a* (mg/m3) = 10^ ((0.015*l3m_day_chlo) – 2.0) (17)

A mask corresponding to the land contours and cloud coverage was applied to all the images in order to exclude these areas in the results, using image processing techniques and overlay operations in ILWIS GIS.

3.2.3 Map projection

The map projection in the output resample maps is based on the Lambert Conformal Conic (LCC) projection within the ISN93 Datum. The central meridian at 19° W, latitude of origin at 65° N and the standard parallels are set to 64° 15´00" N and 65° 45' 00" N as described in "Landmælingar Íslands – Basics on Coordinates and their reference", by Rennen (2002).

3.2.4 In-situ data

In situ Chl and SST data were used to validate the Chl and SST remote sensed information, respectively. *In situ* historical database was obtained from the MRI for the period of May, in the years 2000, 2001 and 2002 for the study area. This information was transformed to point maps and combined with SeaWiFS and NOAA-AVHRR using overlay operation in ILWIS GIS.

3.3 SST and Chl preferences in capelin

The historical CPUE information for the period corresponding to high catches of summer season capelin (July) for the years 2000 to 2002, was combined with NOAA-AVHRR and SeaWiFS images, using overlay procedures to estimate the range of preferences of capelin to the SST and Chl parameters, respectively. Then, these results were fitted to a Gaussian probability distribution and transformed to Fuzzy values, which was used to assign the aptitude values to the study area image according to the evaluated date.

3.4 The GIS-based fishing ground forecasting model

SST and Chl images of 16 July 2003 were the inputs of the model. The previous probability patterns of CPUE with Chl and SST were transformed in Fuzzy values and combined with MCE obtaining just one simple evaluation index. The fuzzy logic is a reasoning procedure that incorporates multiple criteria to evaluate possibilities that each pixel belongs to a Fuzzy set by evaluating any of the series of the Fuzzy set membership functions. A "Fuzzy Set" is a data group described by a function characterized to have values between 0 and 1. By means of this type of functions the factors are standardised to an aptitude scale between 0 (less aptitude) and 1 (high aptitude) (Zadeh 1992, Zadeh 1994, Zimmermann 1987).

Equal weights, which represent the relative importance of each input variable in the solution of the MCE problem, were assigned for the input parameters (SST and Chl). Fuzzy logic operations (Fuzzy AND, Fuzzy OR, Fuzzy algebraic product, Fuzzy algebraic sum and Fuzzy gamma operators) were applied to the final probabilistic map in order to enhance evidences. The resulting fishing ground probability maps were classified into three categories (e.g. "High", "Medium" and "Low" probability), depending on the range of valued obtained. The same procedure was performed using different weights for the input parameters. The SST parameter was proposed to be the highest influence on the spatial distribution of capelin by assigned weights of 0.6 and 0.8.

Additionally, Bayesian probabilistic weights of evidence were generated for the class High probability. The Fuzzy logic was used to obtain the *a priori* probability image; this technique assigns probability values (0 at 1) for each pixel in the evaluated image. To create the conditional probability or evidence images, for SST and Chl, the same previous reasoning is used. An *a- posteriori* probability map was generated using the information of SST and Chl tables in ILWIS, and finally integrated in a MCE procedure. The final map indicated the probability of being a fishing area when evaluating SST and Chl

satellite images. The highest values in the output map were assigned to "High" probability class following the procedure mentioned previously.

4 RESULTS

4.1 Validation of satellite data

SeaWiFS Chl and NOAA AVHRR sea surface temperature were validated with *in situ* information collected by MRI. Some *in situ* Chl values were taken at 0, 10 or 20 m depth. Appendix II and III show the Chl concentration and SST processed images, respectively, both, to validate and for the model implementation. For SST validation, some images were not available for the same period. Figure 7, shows the validation of SeaWiFS (R^2=0.563) and NOAA-AVHRR (R^2=0.87), with *in-situ* information.

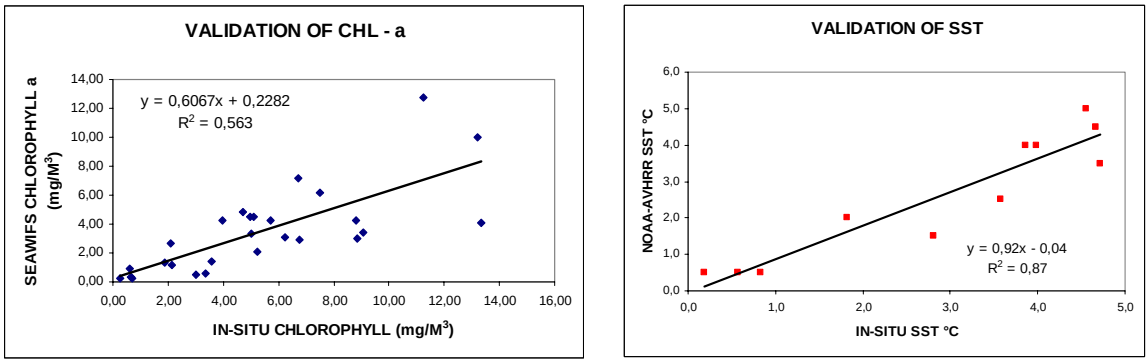

a) *b)*

Figure 6 : Validation of Chl and SST satellite information.

4.2 Fisheries data

From the historical CPUE records of capelin, it was possible to map out the spatial and temporal distribution of this pelagic fish through a frequency analyses. Figure 8, shows the average monthly CPUE of capelin during 1992-2003. The period analysed (July to September) represents the summer season capelin in the north Icelandic waters. CPUE in July was about three times the CPUE in August and September.

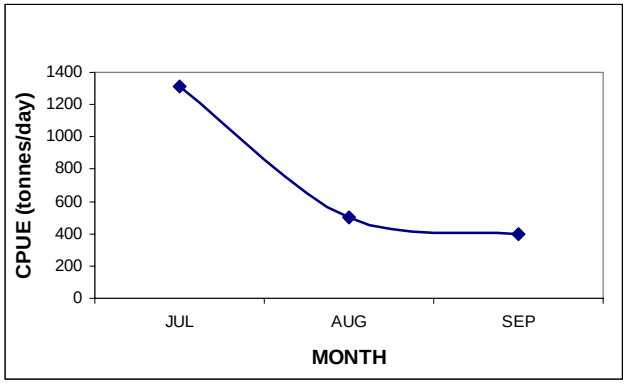

Figure 7: Average monthly CPUE of capelin during 1992-2003.

4.3 Chl, SST and the small pelagic fishery

The CPUE historical database, with catches in July, corresponding to the period of high abundance according to the fishery data, was superimposed with geo-referenced Chl and SST satellite images, using overlay operation in ILWIS GIS. Frequency analysis and probability functions were estimated from this information using the S-PLUS 6.0 (Mathsoft 1998) software. A normal distribution was applied to the CPUE distribution in order to obtain the optimal values for each parameter (Chl and SST) for capelin. These probability distributions were then converted to Fuzzy values to be used in the model. The probability distribution of capelin in July and the optimal range found for each parameter are shown in the Table 9 and Figure 9.

Table 9 : Chl and SST probability distribution for the CPUE information, statistical parameters and optimal, estimated in July.

Parameter	Distribution	N	μ	σ	Interval (mg/m^3)-(°C)	Optimal ranges (mg/m^3)-(°C)
Chl	Normal	51	0,424	0,0442	0,285-1,549	0,2-0,6
SST	Normal	54	4,84	0,8039	2,22-6,0	4,5-6,0

Normal

$$f(x) = \left[1/\left(\sigma * \sqrt{2 * \Pi}\right)\right] * e^{\left[-1/2*((x-\mu)/\sigma)^2\right]}$$

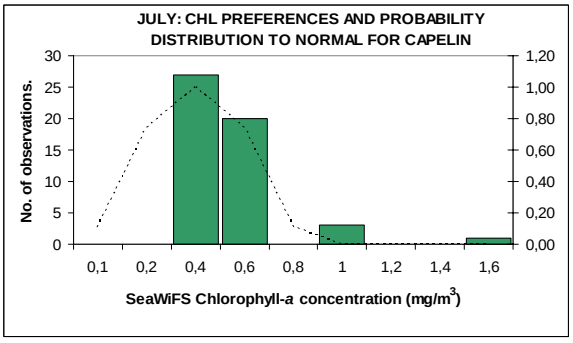

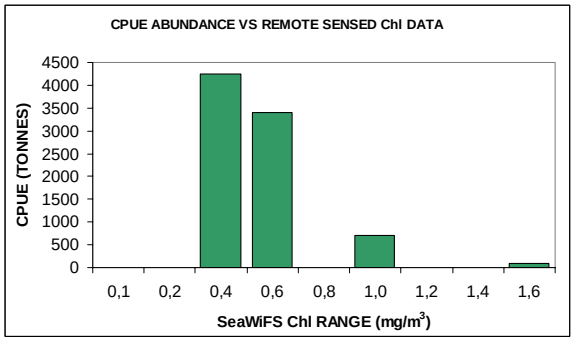

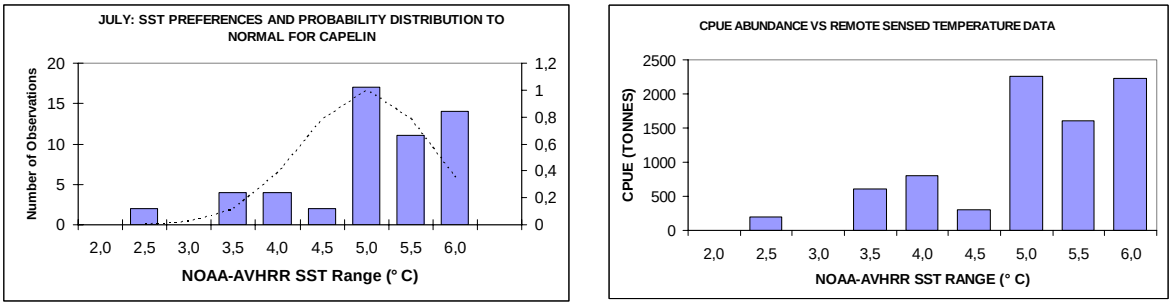

Figure 8: SeaWiFS Chl and NOAA-AVHRR SST probability distribution and CPUE for capelin in July.

4.4 The fishing ground forecasting model for capelin

4.4.1 The image data

Chl and SST images from 16 July 2003 are the inputs of the model. The images were obtained and resampled to be in the same standard coordinate system and pixel size as described in section 3.2.2 (Chl and SST remote sensing images from July 16 2003, are shown in Appendix II and III).

4.4.2 The fishery data

Spatial distribution of catches of capelin in July 2003, was obtained and converted to abundance, expressed in tonnes per square nautical mile. This information was converted to GIF format, and imported to ILWIS GIS for geo-referencing and resembling to be used as an input variable of the model. Figure 10 shows the spatial distribution of the CPUE image of capelin in north Icelandic waters. Catch-per-unit-of-fishing-effort (CPUE) is assumed to be an index of population density and an *a- priori* probability information in the model.

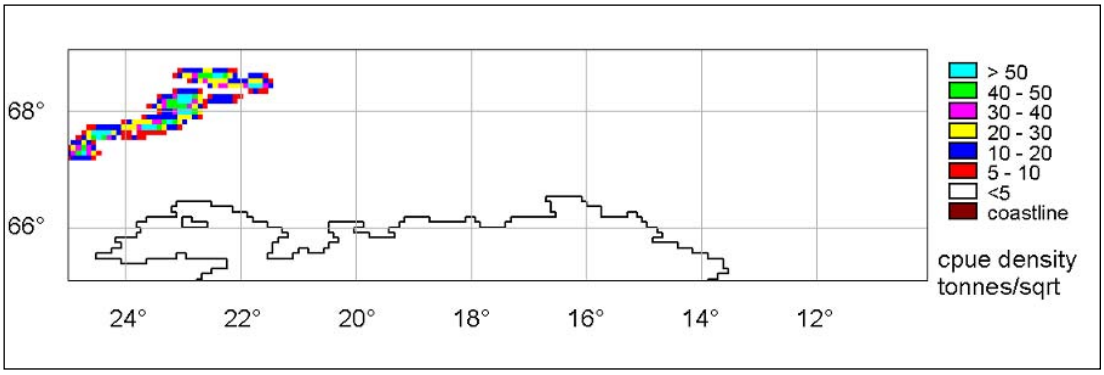

Figure 9: Icelandic CPUE density map of capelin in July 2003. Quantities are expressed in tonnes per square nautical mile**.**

4.4.3 SST and Chl probability maps

Probability maps for spatial distribution of capelin based on both, Chl and SST, were done using the probability distribution and preferences of capelin for Chl and SST parameters, respectively. The probability functions were transformed into Fuzzy values and converted to probability maps based on SeaWiFS Chl and NOAA-AVHRR SST information, and then finally converted into suitability maps by classifying the probability map into three categories of suitability: "Low", "Moderate" and "High" according to the range of values. Figure 11 shows the final Chl and SST probability class maps for capelin in the study area. A mask (in black) that represents land and/or clouds was applied to all images in order to remove the unnecessary values and a contour vector layer (in white) that represent the coastline of Iceland coastline, as well.

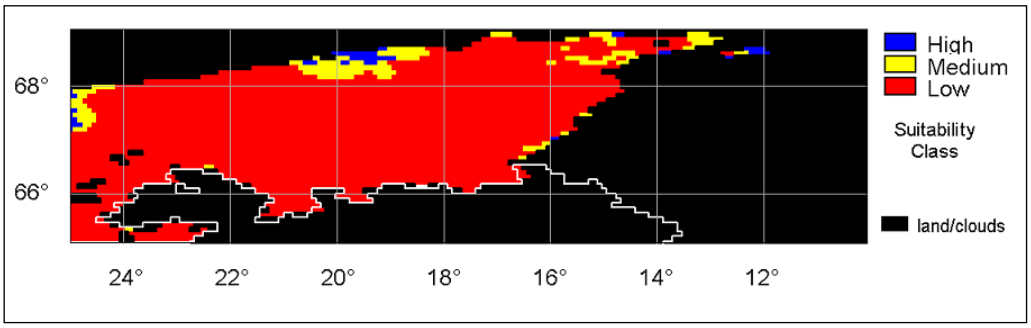

(a)

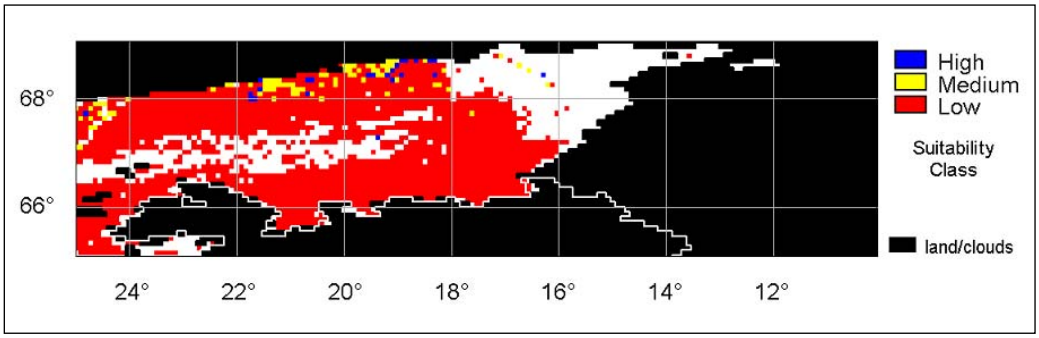

(b)

Figure 10: Probability value maps for capelin based on a) SeaWiFS Chl and b) NOAA-AVHRR.

4.4.4 Knowledge-driven model, weights and probability maps

Two types of approaches were applied to fishing ground forecasting for capelin. These types are described in Table 7. The knowledge-driven approach includes Fuzzy logic operators (Fuzzy OR, Fuzzy AND, Fuzzy Algebraic Product, Fuzzy Algebraic Sum, and Fuzzy Gamma), used to enhance the results. Weights, which represent the importance relative or contribution of each parameter in the solution of the problem, were applied to SST and Chl images as equal (0.5-0.5), and different (0.6-0.4; 0.8-0.2) weights,

respectively, which assume that the SST parameter has higher influence on capelin distribution than Chl. These images were then combined using a Multi-Criteria Evaluation (MCE) technique, with certain combination rules as described in Section 2.4. Figure 12 shows the final probability class maps for capelin, using equal and different weights in the SST and Chl maps. Fuzzy operators were applied only in the equal weights fishing ground forecasting model in order to explore the results as are shown in Figure 13 and Figure 14.

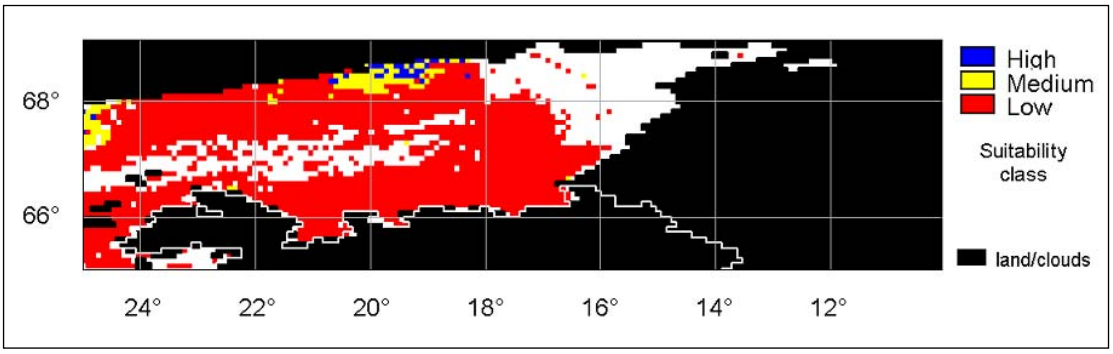

(a)

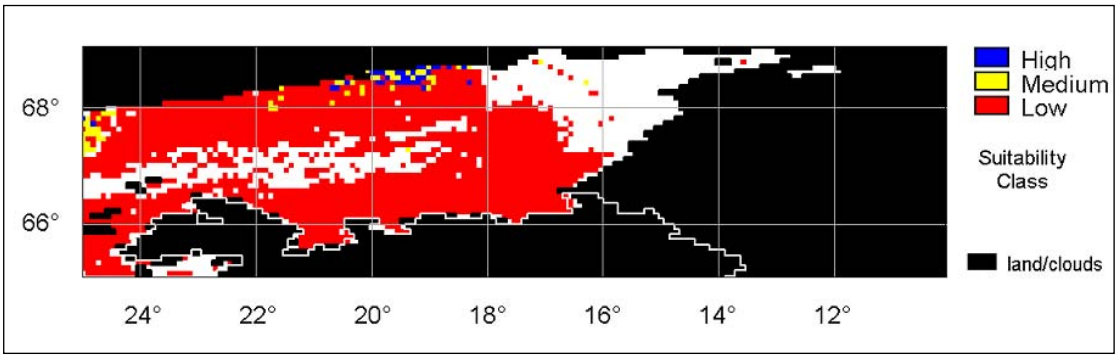

(b)

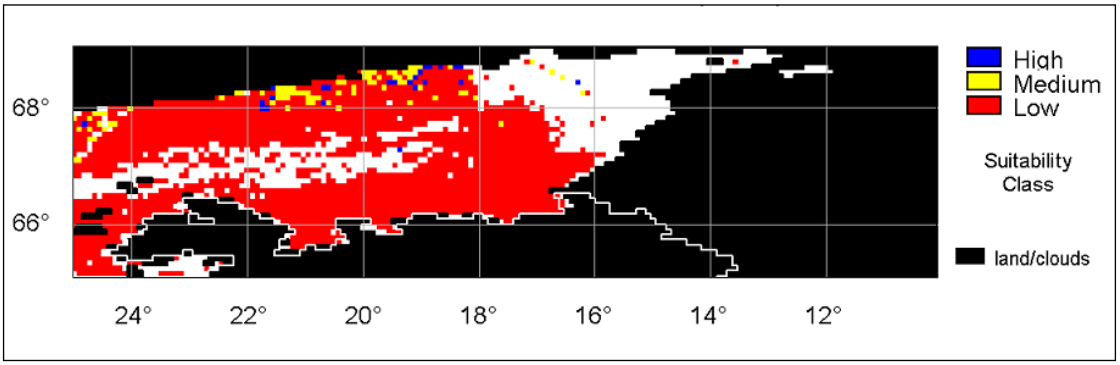

(c)

Figure 11:Probability class maps for capelin using: a) Equal weighs (SST=0.5/Chl=0.5), b) Different weights (SST=0.6/Chl=0.4), and c) Different weights (SST=0.8/Chl=0.2).

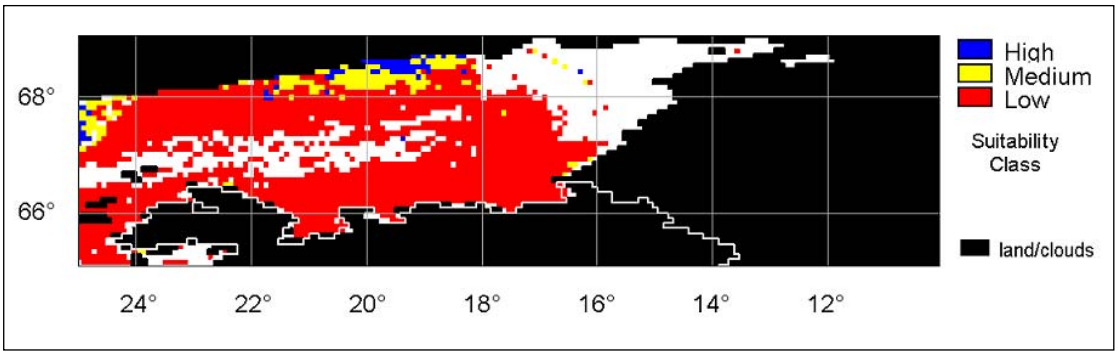

(a)

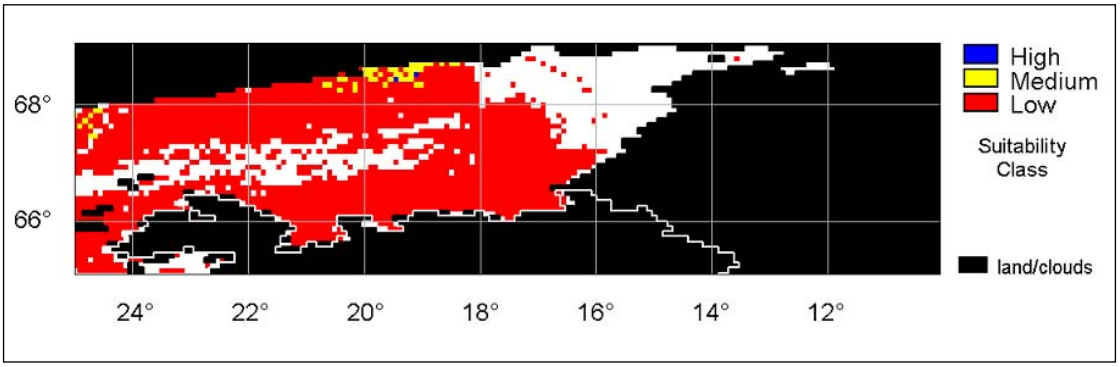

(b)

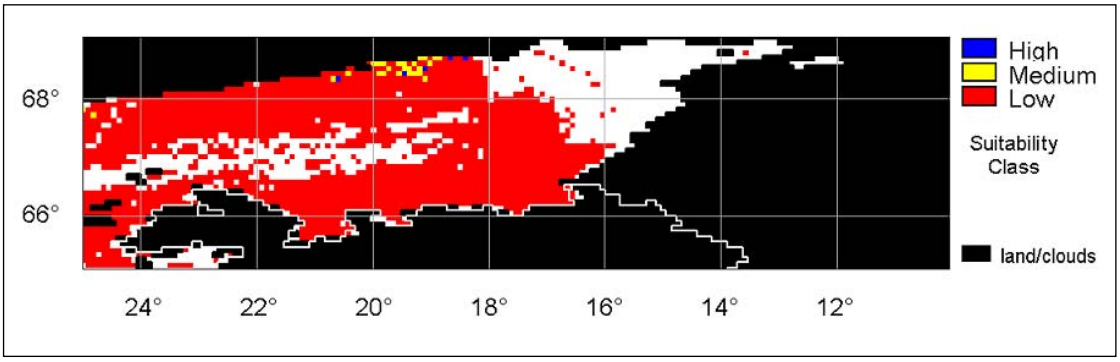

(c)

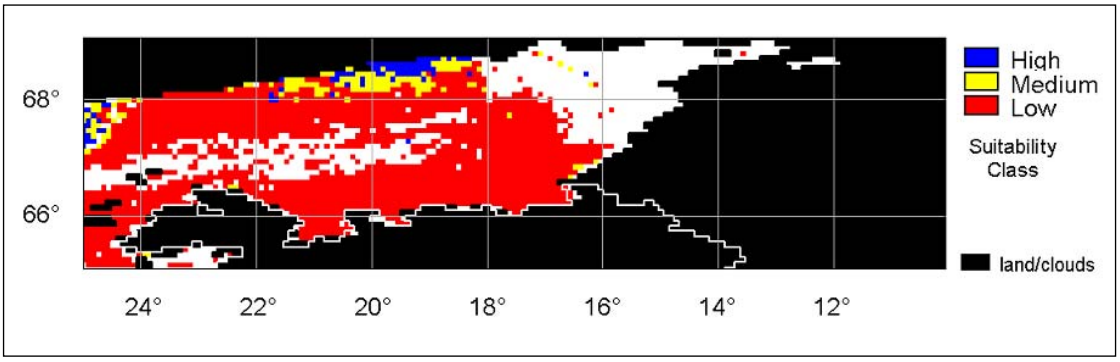

(d)

Figure 12: Probability class maps for capelin using: a) Fuzzy OR, b) Fuzzy AND, c) Fuzzy Algebraic Product, and d) Fuzzy Algebraic Sum.

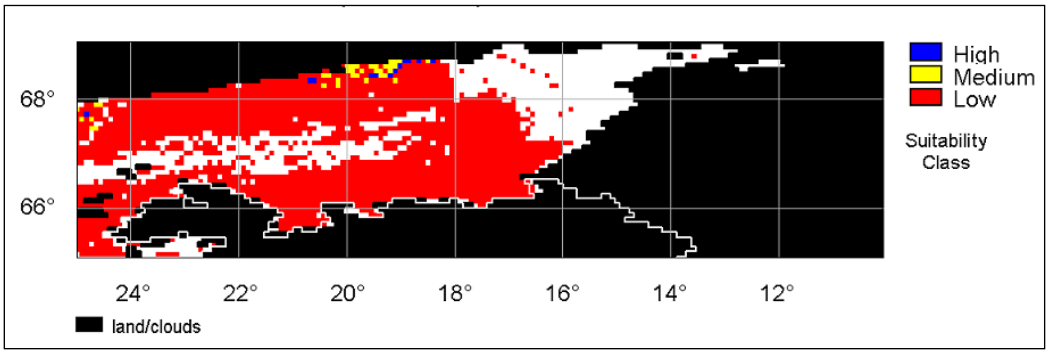

(a)

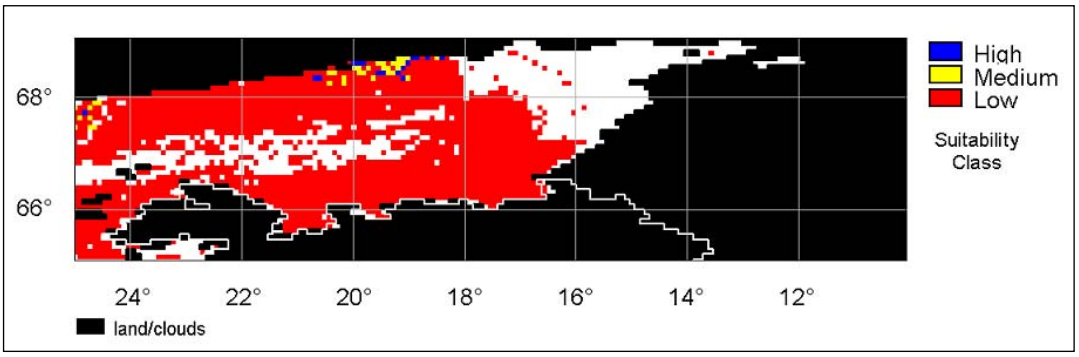

(b)

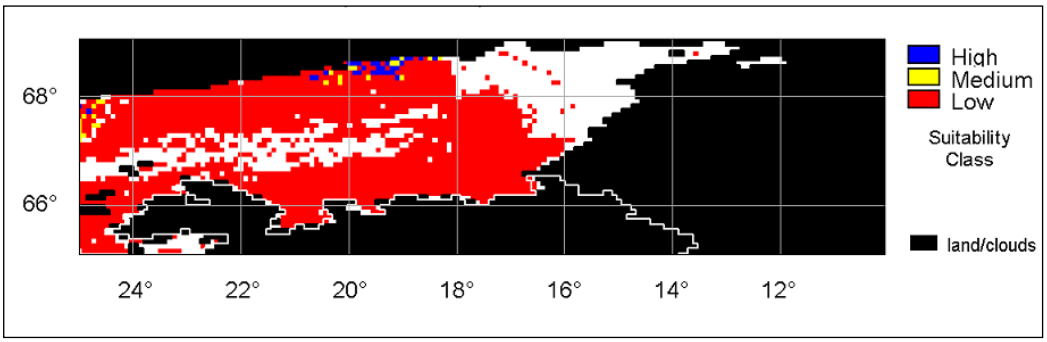

(c)

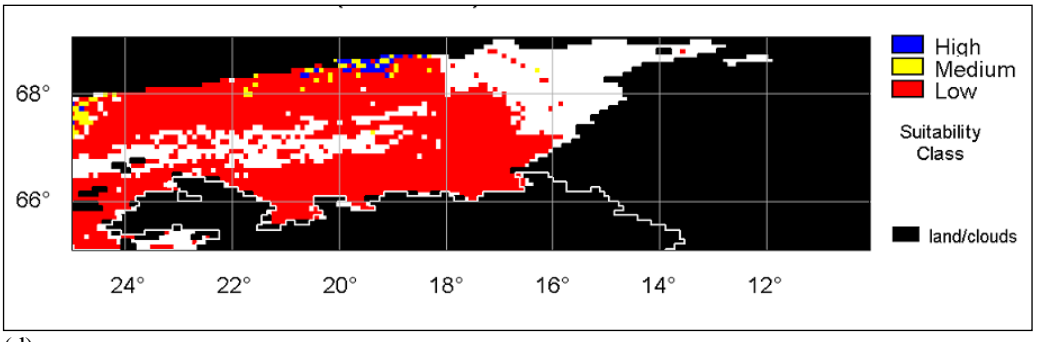

(d)

Figure 13: Probability class maps for capelin using Fuzzy gamma operators: a) gamma=0.2, b) gamma=0.4, c) gamma=0.6, and d) gamma=0.8.

4.4.5 Data-driven model, weights and probability maps

If there is some previous information about a situation to be predicted, the most useful tool used for the evaluation of relationships between indirect evidences and decision-making, is Bayesian Probability Theory (Eastman 1997). It is an extension of the Classical Probability Theory that allows combining new evidence about a hypothesis along with *prior* knowledge (or assumptions) in order to arrive at an estimate of the likelihood of the hypothesis being true. The basis for this is Bayes' Theorem, described in section 2.5.2.

Fuzzy logic is used thorough the modelling process. This technique assigns a probability value (0 at 1) for each pixel in the evaluated image (Zadeh 1992, Zadeh 1994, Zimmermann 1987). For the *a priori* probability image (CPUE map shown in Figure 10), the abundance levels were re-classified into one category. High abundance class in the image was assigned to be > 40 tonnes per square nautical mile. The rest of the categories were assigned into an "unknown" class.

To create the conditional probability images for SST and Chl, the same previous reasoning was used. The application of Bayes' Theorem to each environmental criterion is separately analysed (SST and Chl). SST and Chl values in the images were classified into several classes to produce class maps and then combined with the *a-priori* image in order to obtain the- *posterior* map). This process generated a map that indicates the probability of being a fishing area when evaluating SST and Chl satellite images. An MCE is used to integrate these results using ILWIS GIS software. This procedure assigns weights to the Bayesian results combining the information and finally obtaining just one evaluation index. These values were re-classified into a final probability map with three categories of suitability as seen in Figure. 15.

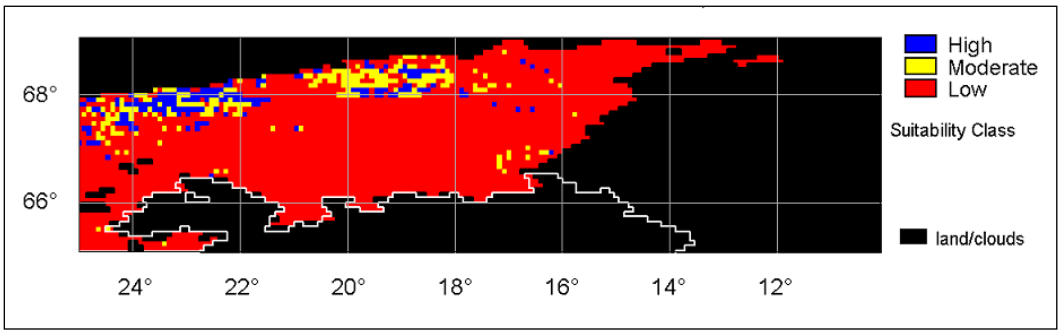

Figure 14: Final potential class map for capelin using Bayes' probabilistic approach.

4.4.6 The model validation

The probabilistic fishing ground maps were validated with geo-referenced CPUE map by performing cross operation in ILWIS GIS. The cross table information of fishing probability class and catches are validated through a frequency analysis, in order to obtain the number of CPUE class pixel, which coincide with the high probability fishing

grounds. Table 10, shows the number of pixels for different suitability classes for all the knowledge-driven models performed. Table 11 and 12, show the number of pixels of CPUE classes which coincide with the "high" probability class for both, knowledge-driven and data-driven models, respectively.

Table 10: Pixel information for knowledge-driven models and percent of total area.

PROBABILITY MAP	PROBABILITY CLASS/No. PIXELS*					
	HIGH	PTA**	MEDIUM	PTA**	LOW	PTA**
NOAA-AVHRR SST.	65	3.05	229	10.76	2277	86.19
SeaWiFS Chl.	62	2.91	216	10.15	2967	86.94
Equal weight (0.5-0.5).	33	1.55	110	5.17	1986	93.28
Diff. weights (0.6-0.4).	63	2.96	162	7.61	1904	89.43
Diff. weights (0.8-0.2).	2	0.09	48	2.25	2079	97.65
Fuzzy OR.	5	0.23	26	1.22	2098	98.54
Fuzzy AND.	80	3.76	145	6.81	1904	89.43
Fuzzy Algebraic Product.	12	0.56	36	1.69	2081	97.75
Fuzzy Algebraic Sum.	16	0.75	35	1.64	2078	97.60
Fuzzy Gamma Operator (0.2).	31	1.46	26	1.22	2072	97.32
Fuzzy Gamma Operator (0.4).	32	1.50	54	2.54	2043	95.96
Fuzzy Gamma Operator (0.6).	32	1.50	57	2.68	2040	95.82
Fuzzy Gamma Operator (0.8)	24	1.13	83	3.90	2022	94.97

* Each pixel represent an approximate area of 8,100 has.
** Percentage of total area.

Table 11: Knowledge-driven validation matrix for the "High" probability class.

PROBABILITY MAP	CPUE CLASS (TONNES PER SQUARED NM) /No PIXELS COINCIDING.						
	< 5	5-10	10-20	20-30	30-40	40-50	> 50
NOAA-AVHRR SST.	57	2	2	2	0	0	1
SeaWiFS Chl.	55	2	1	1	1	1	0
Equal weight (0.5-0.5).	33	0	0	0	0	0	0
Diff. weights (0.6-0.4).	32	0	0	0	0	0	0
Diff. weights (0.8-0.2).	23	1	0	0	0	0	0
Fuzzy OR.	55	3	1	1	1	1	0
Fuzzy AND.	2	0	0	0	0	0	0
Fuzzy Algebraic Product.	5	0	0	0	0	0	0
Fuzzy Algebraic Sum.	69	4	2	2	1	1	0
Fuzzy Gamma Operator (0.2).	12	0	0	0	0	0	0
Fuzzy Gamma Operator (0.4).	16	0	0	0	0	0	0
Fuzzy Gamma Operator (0.6).	31	0	0	0	0	0	0
Fuzzy Gamma Operator (0.8)	32	0	0	0	0	0	0

Table 12: Data-driven validation matrix for the "High" probability class.

CPUE CLASS	PROBABILITY CLASS/No PIXELS		
	LOW	MODERATE	HIGH
High.	22	9	12
Unknown (others)	7452	215	156

5 DISCUSSION

5.1 Validation of satellite data

Validation of remote sensed Chl and SST with *in-situ* data, using a simple linear model, estimated the uncertainly involved as input variables of the fishing ground forecasting model. The validation of the SeaWiFS-derived chlorophyll-a values with concurrent *in situ* measurement showed high correlation in low Chl concentration, but the algorithm used here is not tuned for high Chl concentrations (> 2.5 mg/m^3) (Figure 7a). Similar results were found by Liew (2001), Monirul and Weng (2001), in Singaporean waters and Van Dien *et al.* (2003) in Vietnamese waters, using OC4 to validate the Chl concentration. The remote sensed Chl information, also depends on the algorithm used. In this study, the relations were computed from the digital numbers of the daily SeaWiFS images using the linear equation Chl=10^ ((0.0015*Chl_img)-2.0), included in the HDF file. Those images compute an average of Chl in the grid (9 km x 9 km). The high SeaWiFS-derived Chl values for north Icelandic waters showed a high uncertainty. However, these relations can be useful for further classification in capelin association with low Chl values.

NOAA-AVHRR SST validation with *in-situ* information (Figure 7b) found high correlation. The simple linear model used explained 86% of variability. The algorithm used to extract SST from remote sensing images was the Split Window (McClain *et al.* 1985). The split window technique has been applied extensively to data from the operational NOAA AVHRR series of satellites to provide global estimates of ocean surface temperature. The accuracy of this method is typically of the order of 0.6 - 1.0 degrees Celsius. For tropical regions in particular the atmospheric moisture levels may become very high and the impact on the radiances involved is very significant. Under these conditions a single algorithm may be considerably less accurate with the error in the satellite sensor estimate reaching several degrees C.

It is important to note that the availability of "clean" satellite images (SeaWiFS and NOAA-AVHRR) used for match up analysis with *in situ* measurements was the main problem. Most images from the period May, July 1998-2003 were cloudy in regions, corresponding with *in- situ* information available. It is necessary to obtain more information at different times both, remote sensed and *in-situ* data, in order to improve the reliability of the image calibration.

5.2 Fisheries data

Catch-per-unit-of-fishing-effort (CPUE) in the database is assumed to be an index of population density. CPUE frequency analysis in Figure 8, suggest that the highest abundance of capelin occurs at the beginning of the summer season fishery (July), and decreases rapidly from August to September, as reported by Vilhjálmsson (2002). In addition, great environmental variability in the Icelandic sea is further manifested in catch data from the summer fishing season, showing variations, both of geographic position and catch rates (see Figure 1 in Section 1.4) (Vilhjálmsson 1994). According to

Vilhjálmsson (2002), the most reasonable explanation of the different distribution patterns and variable success of the summer/autumn fishery in those years seem to be environmental variability. Although catches are detected at the end of summer Vilhjálmsson (1994), concluded that the feeding migration of adult capelin to higher latitudes (72° N) during spring and early summer are linked to an east-west temperature gradient. On the other hand, the feeding behaviour is another possible explanation for the capelin abundance and distribution in north Icelandic waters. Capelin feeds on zooplankton, and because of that, capelin abundance seems to be associated with high food availability. In the waters north of Iceland, the spring increase of zooplankton begins at the end of April, reaches a peak in late May and gradually decreases to low winter levels by November (Gíslason and Astthórsson 1996). This seasonal change in the zooplankton biomass is reflected in the feeding activity of the capelin (Astthórsson and Gíslason 1997). This occurs mainly in summer (June-July), when zooplankton populations are high.

5.3 Chl, SST and the small pelagic fishery

For capelin, Chl was in the range of 0,285-1,549 mg/m^3 Chl and the preferred range fluctuates from 0.2 to 0.6 mg/m^3. The SST range is 2.2 to 6.0°C but the preferred range varied from 4.5 to 6.0 °C (Figure 9 and Table 9). Based on the frequency analysis and normal probability distribution, highest abundance of capelin seems to be associated with areas with moderate Chl concentrations from the wide rage of CPUE distribution. Silva *et al.* (2000) found similar results for anchovy (optimal range of 1.2 to 3.1 mg/m^3), sardine (0.7 to 1.3 mg/m^3) and jack mackerel (0.4 to 0.7 mg/m^3) in the north of Chile.

In May the NOAA-AVHRR-derived SST data was fitted to a normal distribution. Also Figure 9 and Table 9, show that capelin is associated with relatively high temperatures during this fishing season. This behaviour is common in pelagic fish as reported by Silva *et al.*, (2000), who found that sardine and jack mackerel are associated with higher temperatures than the anchovy in north of Chile. Similar studies carried out by Barbieri *et al.* (1990) in swordfish (*Xiphias gladius*) in Chile found that the distribution of this pelagic fish is largely influenced by temperature and thermal gradients occurring from March to August, with optimal ranges between 14° to 19° C.

As mentioned before, capelin catches in this area largely depend on hydrologic conditions, which depend on fluctuations in transports and properties of the major current systems in the region, i.e. the supply of warm water masses from the Irminger current, with temperatures ranging from 3-6° C, and cold waters from the east Greenland current that is generally colder than 0°C (Malmberg and Blindheim 1994). On the other hand, the Atlantic ocean provides an important source of nutrients to north of Iceland, because of its relatively high nutrient concentration and the efficiency distribution in the surface layer by eddy diffusion are better than the highly stratified Arctic or polar waters. This makes for a longer-lasting period of phytoplankton production and richer stocks of zooplankton during warm periods than during cold ones (Thórdardóttir 1984 Stefánsson and Ólafsson 1991, Astthórsson and Gíslason 1998) that represent favourable zones for fishing capelin.

Some constraints could be found in the SST, Chl and CPUE data used to estimate the historical relationships, and in the information used to evaluate and validate the model. The low number of images and less cover of the fishing area during May 1998-2003 is the main source of uncertainty in the relationships between capelin distribution and the physical and biological variables (Chl and SST). In the future it is necessary to acquire more daily SST images and daily records of the fleet, for the study period registration of the catch made by the fleet.

5.4 The fishing ground forecasting model for capelin

Each pixel of the SST and Chl images is evaluated by assigning a suitability value from 0 to 1, according to the probability distributions. This classification applying Fuzzy logic allows each pixel to have a suitability value. Knowledge-driven and data-driven models were used for modelling layer information in a MCE.

In the probability image based on SeaWiFS Chl (Figure 11a), areas of high probability are observed between the 67º N and 68º S and 85 to 140 nm offshore the coast, and that zone is favourable for fishing capelin according to Vilhjálmsson (2002). Probability maps based on NOAA-AVHRR SST show that high probability areas were widely distributed and fewer than what was observed based on SeaWIFS (Figure 11b).

Probabilistic maps using equal and different weights obtained in a MCE (Figure 12) were quite similar, both, in spatial distribution and also, in extent. High probability zones were located in the same area as SeaWiFS Chl and NOAA-AVHRR SST-based probability maps. The situation north-eastern of 68º N was more unfavourable, with the high fishing probability areas being 85 - 140 nm off the west coast.

Fuzzy logic operators applied to the knowledge-driven same weight approach, shows large and quite similar high probability areas as using 'OR' and Fuzzy Algebraic Sum operators (Figure 13-(*a)* and –(*d*)). Figure 13-(*b)* and –(c*)* show less extent in the "high" potential class, but also similar to Fuzzy 'AND' and Fuzzy Algebraic Product operators.

The areas predicted as suitable for fishing capelin in the knowledge-driven and data-driven models can be partly verified by the location of existing fishing ground areas (around 68° N and 20°-24° W) and the CPUE map for July 2003 in the area. Comparison has been made also with published data (see Vilhjálmsson 2002). GIS predicted zones with "high" potential close to the existing areas in the north shelf of Iceland. However, there was considerable variation among the predicted and actual locations, possibly due to the 9 km pixel image resolution created both for the NOAA-AVHRR SST and CPUE maps, and also because of the expertise-based weights used. "Medium" and "Low" probability classes in the CPUE evidence map were not considered in the data-driven model because the main goal was to search only for "High" potential.

In the MCE, the linear combination technique can be used to evaluate potential areas for catching capelin. However, the linear weighted combination has several limitations, such as the assumptions of independence and additive of decision variables. In addition the

method does not explicitly deal with spatial context in the decision evaluation; it simply performs localized computations at each spatial location. Two important spatial considerations are to generate coherent spatial areas (Brookes 1997), and to include spatial interactions (Bailey and Gatrell 1995).

Remote sensing applications in fisheries in the region are in its initial stages and there is a lot of potential to expand in the future. This technology promises to improve and to intensify the conventional fishing methods through a good fishing ground forecasting system. However, it is important to note that, in spite of the implementation of these technologies fisheries of capelin will still be totally dependent on local searches (sonar) and stock assessment studies.

5.5 Model validation

It is important to recognise sources of error, which may result from the GIS approach. These may be due to: inaccurate source data, poor parameter choice, and inappropriate SST and Chl remote sensed algorithms and methods. In spite of that, it seems that the findings on capelin in north Icelandic waters agree largely with the spatial and temporal distribution of the catches of capelin in the Iceland-East Greenland-Jan Mayen area in the 1992/1993-2000/2001 fishing seasons, as reported by Vilhjálmsson (2002).

We cannot obviate that model outcomes are subject to certain uncertainty. It resides in the inherent human process for establishing relationship among the direct evidence and the assumed decision, and it should be taken into account. The uncertainty in the model is mainly due to some error in the data source and to the decision rule (Nieto 1999). On the other hand, the number of criteria used to determine the fishing grounds could be insufficient, considering that there are many factors that influence capelin distribution. Although the SST has been demonstrated to be a good indicator of fishing ground in some species such as sardine, anchovy, jack mackerel and swordfish (Nieto 1999, Silva *et al.* 2000, other oceanographic parameters like water masses and oceanic circulation should be included in the model of potential fishing grounds (Nieto 1999).

Since this investigation is still in the experimental stage, the ideas stated in this work are subject to discussion and require further development, *in-situ* validation and implementation.

6 CONCLUSIONS

6.1 Conclusions

The validation of the SeaWiFS-derived Chl values with concurrent *in situ* measurements showed a high correlation in low Chl concentration (however, the algorithm used here is not tuned for high Chl concentrations (> 2.5 mg/m^3)). The NOAA-AVHRR SST validation with *in situ* information also found a high correlation (r^2=0.86).

Capelin was caught in a wide range of Chl (0.285-1.549 mg/m^3) and the preferred range fluctuates from 0.2 to 0.6 mg/m^3. The SST range is 2.2 to 6.0°C but the preferred range is narrower varying from 4.5 to 6.0 °C.

Two approaches were considered to forecast the presence of capelin in north Icelandic waters: knowledge-driven and data-driven models in a Weighted Linear Combination. Weighted Linear Combination techniques, which are flexible in assigning factors, allowing them to compensate for each other, proved to be an effective tool by incorporating more allowance and effectiveness in the suitability analysis of fishing grounds for capelin.

The knowledge-driven model proved to be more flexible and based on expert knowledge than data-driven, which takes into account weights-of-evidence. In all, the fishing grounds forecasting maps for the highest probability of capelin fishing sites were located close to the actual capelin fishing areas of Iceland, between 68°- 69° N and 18°- 25° W, in the shelf north, which has particular hydrological characteristics produced by the convergence of warm North Atlantic waters, and the cold polar waters. Visual interpretation of the results suggest that the fishing ground forecasting model tuned well with the spatial and temporal distribution of the catches of capelin in the north Icelandic waters in the 1992/1993-2000/2001 fishing seasons, as reported by Vilhjálmsson (2002).

Overall, this study has demonstrated the effectiveness of using remotely sensed data in providing the necessary spectral and spatial information for potential fishing grounds. The use of GIS, including a MCE, demonstrated significant capacity for operating a model of fishing ground forecasting for capelin by combining various information layers as well as implementing the necessary analysis on the data.

6.2 Strengths and limitations of this research

6.2.1 Strengths

A major strength of this fishing ground forecasting project was the use of GIS to assess a variety of factors. As with any GIS, the real strength of [the] system comes from combining databases (Kerfoot 1993). The ILWIS program was useful in handling large amounts of data effectively and also, the ability to overlay factors using weightings as well as eliminating areas that are completely unsuitable (mask).

The use of satellite images to extract the parameters Chl and SST, and also, combining GIS and MCE techniques to predict areas with high potential for capelin catches was another strength of this research. Any fishing ground forecasting analysis should include some element of *in-situ* truthing (validation at the sea). As I could not take a trip to north Iceland for validation, the CPUE map from July and also Icelandic figures of capelin catches over several years in the study area were quite useful.

6.2.2 Limitations

Although this particular study achieved the primary objective of creating an operational fishing ground forecasting model through the use of GIS and RS technologies, there are some limitations associated with the research, which should be noted:

The most obvious of these limitations was the specific time constraints, which was the major limiting factor with respect to the depth of research that could be conducted.

The 9 km by 9 km cell size required due to the scale of the SeaWiFS Chl Global Area Coverage (GAC) images was a limitation in the research. A certain amount of generalisation with NOAA-AVHRR SST was required to perform at this resolution, so it could match up with SeaWiFS images. As the project was looking for capelin in north Icelandic waters, limited to some specific areas, the spatial limitation was especially important. Also, the "free of clouds" satellite images availability for these dates was one of the major limitations to validate these images and to perform the model. The amount of variation that can occur within an 81 $(10^{6})$$m^2$ area can be quite significant in the ocean environment.

One of the weaknesses in the research was the inability to obtain geo-referenced SST satellite images from the study area. ILWIS was unable to retrieve geo-referencing of the HRPT LAC images as well. I could not geo-reference these images because I acquired images from a limited area and not enough Ground Control Points were available in those images. As the satellite images are expensive, I only used satellite images available over the Internet free of charge or for a test at Dundee Satellite Station and Freeware to open HRPT images (such as HRPT Reader) was used with the known limitations.

6.3 Recommendations

Despite the study encompassing a sufficient range of criteria; some additions would benefit the practicality of the fishing ground forecasting framework. The inclusion of information such as ecological models, fronts and critical habitat as a constraint, would strengthen the fishing ground forecasting process of our case study because of increased knowledge about the area. Extensive measurements of primary production and also continuous monitoring of fish catches in the north Icelandic waters, when applying the model, would allow using these new evidences to feedback the model in near real-time.

Also it is important to note the significance of planning the fisheries activity in order to develop a long-term plan for access and management of commercial capelin fisheries

based on experience of another similar pelagic fishery such as sardine, in order to assure its sustainability in future years.

Future efforts directed at predicting the abundance and distribution of capelin stocks must give careful consideration to the biotic factors that act on the stock, how they occur, and what the force function is. Without an understanding of the dynamics of the biota/environment link we will never progress from statistical or empirical models to conceptual and mechanistic models.

ACKNOWLEDGEMENTS

Over several months, I participated in an intensive course at the UNU/FTP in Iceland. After that, I applied my skills on GIS and RS to pelagic fishing ground forecasting in the north of Iceland as a case study. During the elaboration of the present research, I have received encouragement and assistance from different sources.

I like to express my sincere gratitude to the Government of Iceland, especially to UNU for their kindness and fellowship to undertake my studies. Also, to all staff of the Marine Research Institute (MRI), for their assistance and the supply of data. I very much enjoyed the white and fresh landscape there, since I no longer live in Iceland. They brought beautiful memories of a land filled with wonderful, friendly, kind and respectful people.

I would like to thank my supervisors -Dr. Geir Oddsson, and -Dr. Héðinn Valdimarsson,the main guides in my studies, - Dr. Ólafur S. Astthórsson, for his comments on the Icelandic capelin and climatic conditions; -Dr Kristinn Guðmundsson, for his assistance on providing in situ Chl-*a* data and suggestions; -Dr Höskuldur Björnsson for providing me a capelin fishing ground map of Iceland; -Dr Sigfús Jóhannesson for his help in data management and for his assistance on the capelin CPUE database; and Dr. Hjálmar Vilhjálmsson for his valuable comments and data support on capelin.

In addition, I would like to thank Dr. Tumi Tómasson, director of UNU/FTP for his assistance and friendship during my studies in Iceland. Mr. Þór Ásgeirsson, for his valuable guide in my studies and friendship and who spent many hours checking my progress in the training course and final reports.

I would like to acknowledge the assistance of Jónas Jónasson, and James Begley at MRI, for their valuable assistance. Also thanks to Ingibjörg Jónsdóttir at the Iceland University and Neil Lonic at the NERC Satellite Receiving Station at University of Dundee for providing me MODIS and NOAA-AVHRR images and for their support and comments.

I would like to thank the SeaWiFS Project (Code 970.2) and the Distributed Active Archive Center (Code 902) at the Goddard Space Flight Centre (Greenbelt, MD 20771) for the production and distribution of these data, respectively. These activities are sponsored by NASA's Mission to Planet Earth Program.

LIST OF REFERENCES

Aijad, A., and Pushchaeva, T.A. 1992. Daily feeding dynamics of the Barents Sea capelin from different size groups during the feeding period. *In* Investigations of Fish Population Interrelations in the Barents Sea, pp. 262-285. Proceedings of the Fifth Soviet-Norwegian Symposium, Murmansk.

Amidei, R., Ed. 1983. Applications of remote sensing to fisheries and coastal resources. Report of a California Sea Grant workshop. Report No. T-CSGCP-012

Anon. 1993. International Workshop on Application of Satellite Remote Sensing for Identifying and Forecasting Potential Fishing Zones in Developing Countries. Organized by Department of Space, National Remote Sensing Agency (NRSA), Hyderabad and Committee on Science and Technology in Developing countries of the International Council of Scientific Unions (Coasted/ICSU), Madras, Hyderabad, India. 7-11 Dec. 1993.

Ástþórsson, Ó. S., Hallgrímsson, I., and Jónsson, G.S. 1983**.** Variations in zooplankton densities in Icelandic waters in relation to environmental conditions. ICES Mar. Sci. Symp., 198:529-541.

Ástþórsson, Ó. S., and Gíslason, A. 1997. On the food of capelin in the subartic waters north of Iceland. Sarcia 82:81-86. Bergen. ISSN 0036-4827.

Ástþórsson, Ó. S., and Gíslason, A. 1998. Environmental conditions, zooplankton and capelin in the waters north of Iceland. ICES Journal of Marine Science, 55: 808-810.

Barbieri, M.A., E. Yáñez, L. Aríz y A. González. 1990. La pesquería del pez espada: tendencias y perspectivas. *In*: Perspectivas de la Actividad Pesquera en Chile. M.A. Barbieri (Ed.), Escuela de Ciencias del Mar, UCV, Valparaíso, Chile: 195-214.

Bonham-Carter, G.F., 1999. Geographic Information Systems for Geoscientists. Modelling with GIS. Computer Methods in the Geosciences, 13:pp 267-302. Pergamon. CITED AS BONHAM-CARTER 1998!

Brookes, C.J. 1997. A parameterized region-growing programme for site allocation on raster suitability maps. International Journal of Geographic Information Systems, Vol.11 (4), pp.375-396.

Burrough, P.A. and McDonnel, R.A.. 1998. Principles of Geographical Information Systems, Oxford University Press, Oxford, 333 pp.

Caddy, J.F. and Carocci, F. 1999. The spatial allocation of fishing intensity by port-based inshore fleets: a GIS application. ICES Journal of Marine Science, 56: 388-403

Carscadden, J.E., Frank, K.T., and Miller, D.S. 1989. Capelin (*Mallotus villosus*) spawning on the southeast shoal: influence on physical factors past and present. Canadian Journal of Fisheries and Aquatic Sciences, 46: 1743-1754.
Carver, S.J. 1991. Integrating Multi-Criteria Evaluation with Geographical Information Systems. In: International Journal of Geographical Information Systems, 5(3):321-339.

Chrisman, L. 1991. Learning recursive distributed representations for holistic computation. Connection Science, 3, 345—365.

COMS (Center for Ocean Management Studies). 1978. Climate and Fisheries. Proceedings from a workshop on the influence of environmental factors on fisheries production. University of Rhode Island. Kingston, Rhode Island. P.2.

Curran, P.J. 1985. Principles of Remote Sensing. Longman. London.

Eastman, J. R. 1997. Multi-Criteria Evaluation - Boolean and Weighted Linear Combination. In Tutorial Exercises: Idrisi for Windows Version 2.0. Clark Labs for Cartographic Technology and Geographic Analysis. Adv-24 to Adv-34.

Fernández, E., and R.D. Pingree. 1996. Coupling between physical and biological fields in the North Atlantic subtropical front southeast of the Azores. Deep-Sea Res. 43(9): 1369.

Gíslason, A. and Ástþórsson, Ó.S. 1996. Seasonal variations in biomass, abundance and composition of zooplankton north of Iceland. –ICES Council Meeting 1996/L:26. 15 pp. Biological Oceanographic Committee.

Glantz, M.H. and Geingold, L. E. 1990. Climate Variability, Climate Change and Fisheries. Environmental and Societal Impacts Group. National Center for Atmospheric Research. Boulder, Colorado. Pp. 103-107

Goddard, S.V., Kao, M.H., and Fletcher, G.L. 1992. Antifreeze production, freeze resistance and over wintering of juvenile northern Atlantic cod (*Gadus morhua*). Can. J. Fish. Aquat. Sci., 49:516-522.

González, A. 1993. Distribución espacio-temporal de la pesquería artesanal de pez espada (*Xiphias gladius*) desarrollada por la flota artesanal de Valparaíso y variaciones ambientales entre 1987 y 1991. Tesis para optar al título de Ingeniero Pesquero, Escuela de Ciencias del Mar, UCV, Valparaíso, 94 pp.

ICES 2000. Report of the Northern Pelagic and Blue Whiting Working Group. ICES CM 2000/ACFM: 16, 100-118.

Iluz, D., Yacobi, Y. Z. and Gitelson, A.. 2003. Adaptation of an algorithm for Chlorophyll-estimation by optical data in the oligotrophic Gulf of Eilat. Int. J. Remote Sensing. Vol. 24, No. 5, 1157–1163.

Jakobsson, J. 1992. Recent variability in the fisheries of the North Atlantic. ICES Mar. Sci. Symp. 195:291-315.

Jankowski, P. 1995. Integrating geographical information systems and multiple criteria decision-making methods, International Journal of Geographical Information Systems, 9(3), 251-273.

Janssen, R., Rietveld, P. 1990. Multi criteria analysis and GIS: an application to agricultural land use in the Netherlands, In , Geographical Information Systems for Urban and Regional Planning, Eds. Scholten, H.J., Stillwell, J.C.H., Kluwer : Dordrecht.

Jiang, H., and Eastman, J.R. 2000. Application of Fuzzy Measures in Multi-Criteria Evaluation in GIS, International Journal of Geographic Inf. Science, 14,2,173-184.

Kanthi, K.Y. 2000. Seasonal variability of sea surface chlorophyll-a of waters around Sri Lanka. Proc. Indian Acad. Sci. (*Earth Planet. Sci*.), 109, No. 4. pp. 427-432.

Laurs, R. M. 1993. Integration of various satellite derived oceanography information for the identification of potential fishing zones. In *Lecture notes of International workshop on application of satellite remote sensing for identifying and forecasting potential fishing zones in developing countries*, Hyderabad, India, 7-11 December 1993.

Liew, S.C. Chia, A.S., Kwoh, L.K.. 2001. Evaluating the vality of SeaWiFS chlorophyll algorithm for coastal waters. 22nd Asian Conference on Remote Sensing, 5-9 November 2001, Singapore.

Lillesand, T. M. and Kiefer, R. W.. 2000. Remote sensing and image interpretation. New York ; Chichester England, Wiley.

Linnaeus, C. 1758. Systema Naturae, Ed.X. (Systema naturae per regna tria naturae, secundum classes, ordines, genera, species, cum characteribus, differentiis, synonymis, logis. Tomus I. Editio decima, reformata.) Holmiae. Sistema Nat. Ed. 10 i-ii + 1-824. CAS Ref No. 2787. Nantes and Pises in Tom. 1 pp. 230-335; a few species on later pages. Date fixed by ICZN, Code Article 3.

Malmberg, S.A. 1986. The ecological impact of the East Greenland Current on the North Icelandic waters, NATO ASI series Vol. G7, 389-404.

Malmberg, S.A., and Blindheim, J. 1994. Climate, cod and capelin in northern waters. ICES Marine Science Symposia, 198:207-310.

Mansor, S., Tan, C. K., Ibrahim, H.M. and Shariff, A.R.M. 2001. Asian Conference on Remote Sensing. 5-9 November 2001. Asian Association on Remote Sensing (AARS). Singapore.

Mathsoft, 1998. S-PLUS 6.0. Statistical software. The Mathworks.

McAllister, D.E. 1964. A revision of the smelt family, Osmeridae. National Museum of Canada Bulletin, 191. 53 pp.

McClain, E.P., Pichel, W.G., and Walton, C. C.. 1985. Comparative performance of AVHRR-based multichannel sea surface temperature. J. of Geophysical research, vol. 80, pp. 5113-5117.

Monirul, M.I., and Chang W. T. 2001. A comparison of empirical algorithms for chlorophyll concentration in Singapore regional waters. 22nd Asian Conference in Remote sensing, 5-9 November 2001.

Nakashima, B.S., and Wheeler, J.P. 2002. Capelin (*Mallotus villosus*) spawning behaviour in Newfoundland waters – the interaction between beach and demersal spawning. ICES Journal of Marine Science, 59:909-916.

Nieto, K. 1999. Determinación de zonas probables de pesca de pez espada (*Xiphias gladius*) en Chile central, a través de imágenes de temperatura superficial del mar de satelites NOAA. Tesis para optar al título de Ingeniero Pesquero, Escuela de Ciencias del Mar, UCV, Valparaíso, 92 pp.

O'Brien, J.J., Woodworth, B.M., and Wright. 1974. The Coho Project (Living Resources Prediction Feasibility Study) Reports. Vol. I, Final Report Vol. II, Environmental Report; and Vol. III, System evaluation report. School of Oceanography, Oregon State Univ, Corvallis. Ore.

Olson, D.B., Hitchcock, G.L., Mariano, A.J., Ashjian, C.J., Peng, G., Nero, R.W. and Podesta, G.P.. 1994. Life on the edge: Marine Life and fronts. Oceanography. 7(2): 52-60

O'Reilly J.E., Maritorena S., Mitchell, B.G., Siegel, D.A., Carder, K.L., Garver, S.A., Kahru, M., and McClain, C. 1998. Ocean color chlorophyll algorithms for SeaWiFS. Journal of Geophysics Research. 103c, pp. 24937-24953.

O'Reilly, Maritorena, J.E., Siege, S. D., M.O´Brien, D. Toole, B. Mitchell, G., Kahru, M., Chavez, F., Strutton, P., Cota, G., Hooker, S.. McClain, C., Carder, K., Muller-Karger, F., Harding, L., Magnuson, A., Phinney, D., Moore, G., Aiken, J., Arrigo, K., Letelier, R. and Culver, M.. 2000. Ocean color chlorophyll a algorithms for SeaWiFS, OC2, and OC4: Versión 4. *In*: O'Reilly, J.E., and 24 co-authors, 2000: SeaWiFS postlaunch Calibration and Validation Analyses, Part 3. NASA Tech. Memo. 2000-2066892, Vol. 11, S.B. Hooker and E.R. Firestone, Eds., NASA Goddard Space Centre, Greenbelt, Maryland, 9-23.

Pálsson, Ó. K. 1983. The Feeding habits of demersal fish species in Icelandic waters. Rit Fiskideildar, VII (1) 60 pp.

Panasenko, L.D. 1984. Feeding of the Barents Sea capelin. ICES Council Meeting 1984/H:6, 12 pp. Pelagic Fish Committee.
Panasenko, L.D. 1989. Daily variations in feeding and rations of the Barents Sea capelin (*Mallotus villosus*) in summer-autumn period. In Daily Rhythms and Rations of Feeding of Commercial Fishes in the World Ocean, pp.63-75.VNIRO, Moscow.

Podesta, G. P., Browder, J. A. and Hoey, J. J. 1993. Exploring the association between swordfish catch and thermal fronts on the US long-line grounds in the western North Atlantic. Cont. Shelf. Res. 13: 253-277.

Polovina, J.J. 1997. Local-scale swordfish fisheries oceanography. In: Second international Pacific Swordfish symposium, Hawaii, March 3-6.

Rennen, M. 2002. Basic on coordinates and their reference. Landmælingar Íslands.

Saaty, T.L. 1977. A scaling method for priorities in hierarchical structures. Journal of Mathematical Psychology 15, 234-281.

Shafer, G., 1976. A Mathematical Theory of Evidence. Princeton University Press, New Jersey.

Silva, C., Yáñez, E., Barbieri, M.A., Nieto, K., Mimica, V., Espíndola, F. and Acevedo, J. 2000. Sixth International Conference on Remote Sensing for Marine and Coastal Environments, Charleston, South Carolina, 1-3 May, 2000.

Simpson, J.J. 1992. Remote sensing and geographic information systems: implications for global marine fisheries. A publication of the California Sea Grant College, Report No. T-CSGCP-025.

Simpson, J.J. 1994. Remote sensing in fisheries: a tool for better management in the utilization of a renewable resource. Canadian Journal of Fisheries and Aquatic Sciences, 51: 743-771.

Skoldal, H., Gjosæter, H., and Loeng, H. 1992. Ecosystem of the Barents Sea in the 80s: climatic changes, plankton and capelin growth. Investigations of interrelations between fish populations in the Barents Sea, pp. 318-339. Selected papers, Soviet-Norwegian Symposium, Murmansk.

Stefánsson, U., and Ólafsson, J. 1991. Nutrients and fertility of Icelandic waters. Rit Fiskideildar, 12:3:1-56 pp.

Stefánsson, U., and Ólafsson, J. 1992. Nutrients and fertility of Icelandic waters. Rit Fiskideildar, 12:1-56.

Steinarsson, B.Æ., and Stefánsson, G. 1991. An attempt to explain cod growth variability. ICES CM 1991/G:42.

Taylor, C., Bigelow, H. B. and Graham, H. W. 1953. Climate Trends and Distribution of Marine Animals in New England. U.S. Fish and Wildlife Service, Fishery Bulletin 115 (Vol. 57): pp. 293-345.

Thórdardóttir, Th. 1984. Primary production north of Iceland in relation to water masses in May-June 1979-1980. ICES CM 1984/L:20

Tomlin, C.D. 1991. Cartographic Modelling, *In*: D. Macguire, M Goodchild and D. Rhind, Longman (eds) Geographical Information Systems, 1, 361-374.

Van Dien, Tang, T. D.L., Kawamura, H.. 2003. Validation of SeaWiFS-derived ocean color data and using for study distribution and seasonal variation of Chlorophyll-a concentration in the Vietnam waters. Remote sensing and Geographic Information Systems (GIS) Applications for sustainable development. 81, 82-89

Vilhjálmsson, H. 1983. Biology, abundance estimates and management of the Icelandic stock of capelin.- Rit Fiskideildar 7:153-181.

Vilhjálmsson, H. 1984. The Icelandic capelin stock. Capelin *Mallotus villosus* (Muller) in the Iceland, Greenland, Jan Mayen Area. Rit Fiskideildar 13:281 pp.

Vilhjálmsson, H. 1994. The Icelandic capelin stock. Capelin Mallotus villosus (Muller) in the Iceland, Greenland, Jan Mayen area. Rit Fiskideidar, 13:281 pp.

Vilhjálmsson, H., and Carscadden, J.E. 2002. Assessment surveys for capelin in the Iceland-East Greenland-Jan Mayen area, 1978-2001.-ICES Journal of Marine Science, 59:1096-1104.

Vilhjálmsson, H. 2002. Capelin (*Mallotus villosus*) in the Iceland-Greenland-Jan Mayen ecosystem. ICES Journal of Marine Science, 59: 870-883.

Voogd, H., 1983. Multicriteria Evaluation for Urban and Regional Planning. Pion, London. World Commission on Environment and Development (WCED). 1987. Our Common Future. Oxford University Press, Oxford.

Westen, C.J. 2001. Statistical landslide hazard analysis. Training package for Geographic Information System. Chapter 05. ITC-Publication Number 5, ITC, Enschede, The Netherlands. 73-84.

Yáñez E., Silva, C., Barbieri, M. A. and Nieto, K.. 1996. Pesquería artesanal de pez espada y temperatura superficial del mar registrada con satélites NOAA en Chile central. Invest. Mar., Valparaíso, 24: 131-144.

Yáñez E., Barbieri, M.A., Silva, C. and Nieto, K.. 1997. Oceanography and the swordfish fishery in Chile. *In*: Second international Pacific Swordfish Symposium, Hawaii, March 3-6.

Zadeh, L. A. 1992. Fuzzy Sets. In: Readings in Fuzzy Sets for Intelligent Systems. D. Dubois, H. Prade, and R. Yager, Morgan Kaufmann (Ed), San Mateo, CA.

Zadeh, L. A. 1994. Fuzzy Logic, Neural Networks, and Soft Computing. Communications of the ACM, 37(3): 77 - 84.

Zheng X., Pierce G.J., Reid D.G., Jolliffe I.T. 2002. Does the North Atlantic current affect spatial distribution of whiting? Testing environmental hypotheses using statistical and GIS techniques. ICES Journal of Marine Science, April 2002, vol. 59, no. 2, pp. 239-253(15).

Zhou, Q. 1995. Introduction to Geographic Information Systems. Proceedings of United Nation ESCAP Workshop on Remote Sensing and GIS for Land and Marine Resources and Environment Management, 13-17 February, Suva, Fiji. Pp 28-42.

Zimmermann, H. J. 1987. Chapter 1 - Introduction, Fuzzy Sets, Decision Making, and Expert Systems, Kluwer Academic Publishers, Boston, 1 - 14.

Web sites.
http://www.sat.dundee.ac.uk/projections.html (nov-dec 2003).
http://www.niwa.co.nz/pubs/wa/09-1/front.htm (dec-22-2003).
http://www.makalu.com.mx/antartica/cartografiapolos.html (dec-12-2003).
http://www.pcigeomatics.com (nov-24-2003).
http://swfsc.nmfs.noaa.gov/fish_res.html (nov-15-2003).
http://modis.gsfc.nasa.gov/data/atbd/atbd_mod19.pdf (dec-15-2003).
http://www.marine.usm.edu/syllabus/MAR602lecture14-2002.htm. (dec-22-2003).
http://www.cig.ensmp.fr/~iahs/sapporo/abs/jsg03/017418-1.html (feb-07-2004).

APPENDIX I: COEFFICIENTS FOR SEA SURFACE TEMPERATURE ALGORITHMS

Table 13: Coefficients for split-window algorithm.

Satellite	Time	A_0	A_1	A_2	A_3	A_4(K)	A_4(C)
NOAA-14	D	1.017342	2.139588	0.779706	0.000	-5.280	-0.543
NOAA-14	N	1.029088	2.275385	0.752567	0.000	-9.090	-1.145
NOAA-12	D	1.013674	2.443474	0.314312	0.0	-4.647	-0.912
NOAA-12	N	1.013674	2.443474	0.314312	0.0	-4.647	-0.912
NOAA-11	D	1.01345	2.659762	0.526548	0.0	-4.592	-0.918
NOAA-11	N	1.052	2.397089	0.959766	0.0	-15.52	-1.316
NOAA-9	D	0.9994	2.7057	-0.27	0.73	0.1177	-0.046
NOAA-9	N	0.9994	2.7057	-0.27	0.73	0.1177	-0.046
NOAA-7	D	1.0346	2.5779	0.0	0.0	-10.05	-0.60
NOAA-7	N	1.0346	2.5779	0.0	0.0	-10.05	-0.60
NOAA-10	D	1.1	0.0	0.0	0.0	-27.316	0.0
NOAA-10	N	1.1	0.0	0.0	0.0	-27.316	0.0
NOAA-8	D	1.1	0.0	0.0	0.0	-27.316	0.0
NOAA-8	N	1.1	0.0	0.0	0.0	-27.316	0.0
NOAA-6	D	1.1	0.0	0.0	0.0	-27.316	0.0
NOAA-6	N	1.1	0.0	0.0	0.0	-27.316	0.0

Table 14: Coefficients for dual-window algorithm.

Satellite	Time	A_0	A_1	A_2	A_3	A_4(K)	A_4(C)
NOAA-14	N	1.008751	1.409936	0.000000	1.976	-0.764	1.626
NOAA-12	D	1.017736	0.426593	1.800916	0.0	-3.114	1.731
NOAA-12	N	1.017736	0.426593	1.800916	0.0	-3.114	1.731
NOAA-11	D	1.03432	1.347423	0.953042	0.0	-7.64	1.73
NOAA-11	N	1.03432	1.347423	0.953042	0.0	-7.64	1.73
NOAA-9	D	1.014	0.5118	0.958	1.55	-2.224	1.60
NOAA-9	N	1.014	0.5118	0.958	1.55	-2.224	1.60
NOAA-10	D	1.009	1.502	0.0	-1.2	-2.58	-0.12
NOAA-10	N	1.009	1.502	0.0	-1.2	-2.58	-0.12
NOAA-8	D	1.009	1.502	0.0	-1.2	-2.58	-0.12
NOAA-8	N	1.009	1.502	0.0	-1.2	-2.58	-0.12
NOAA-7	D	1.009	1.502	0.0	-1.2	-2.58	-0.12
NOAA-7	N	1.009	1.502	0.0	-1.2	-2.58	-0.12
NOAA-6	D	1.009	1.502	0.0	-1.2	-2.58	-0.12
NOAA-6	N	1.009	1.502	0.0	-1.2	-2.58	-0.12

Table 15: Coefficients for triple-window algorithm.

Satellite	Time	A_0	A_1	A_2	A_3	A_4(K)	A_4(C)
NOAA-14	N	1.010037	0.920822	0.000000	1.760	2.214	0.528
NOAA-12	N	1.058532	1.016347	0.0	2.081917	-3.407	12.58
NOAA-11	N	1.036027	0.892857	0.520056	0.0	-9.224	0.617

APPENDIX II: SEAWIFS IMAGES WITH CHL CONCENTRATION

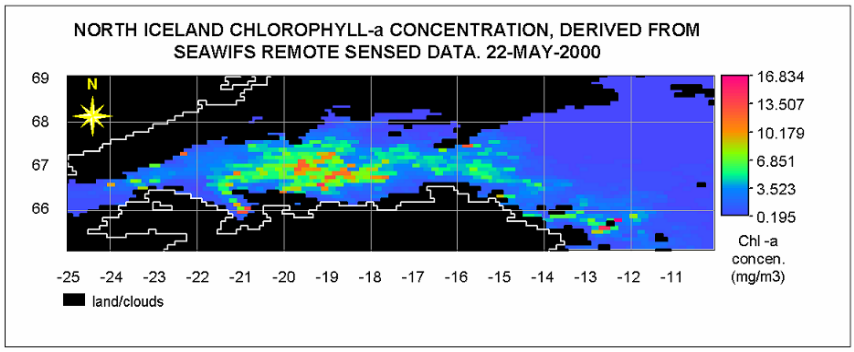

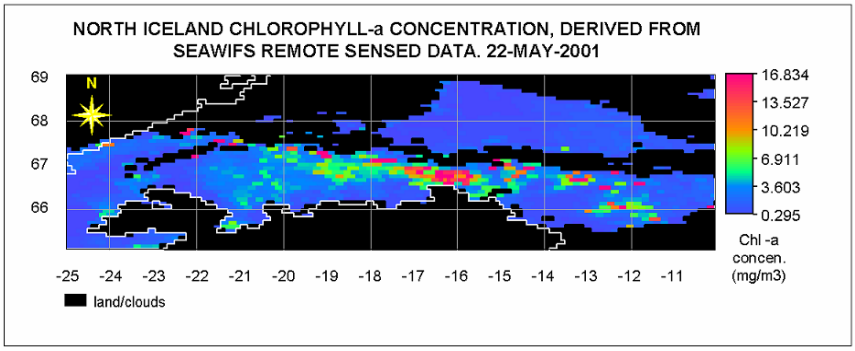

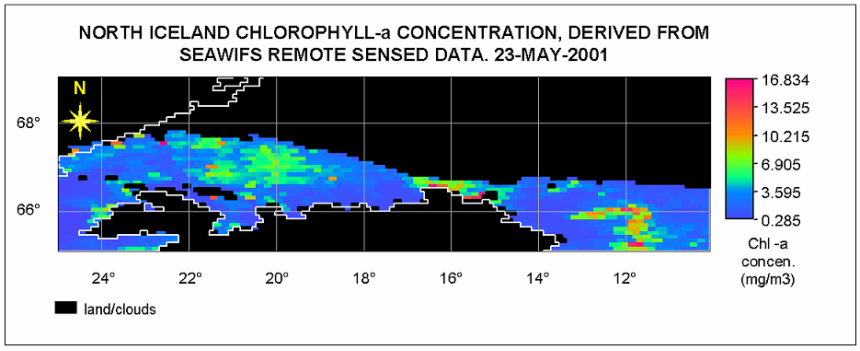

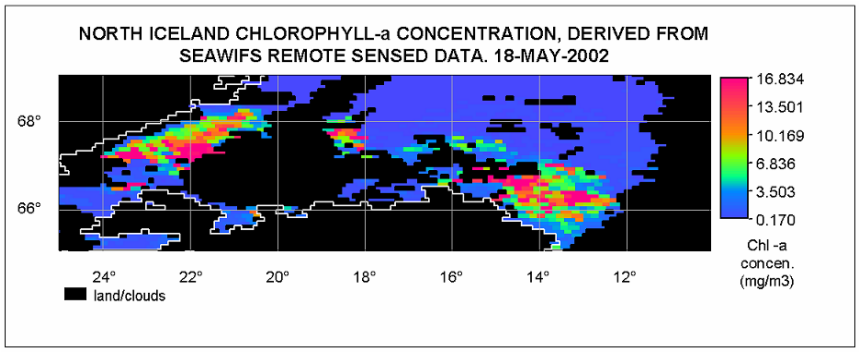

APPENDIX III: NOAA-AVHRR SST IMAGES WITH SST CLASS